Resonant homoclinic flip bifurcations

Ale Jan Homburg
Institut für Mathematik I
Freie Universität Berlin
Arnimallee 2–6
14195 Berlin
Germany
alejan@math.fu-berlin.de

Bernd Krauskopf
Physics and Astronomy
Vrije Universiteit
De Boelelaan 1081
1081 HV Amsterdam
The Netherlands
berndk@nat.vu.nl

August 1998

Abstract

This paper studies three-parameter unfoldings of resonant orbit flip and inclination flip homoclinic orbits. First all known results on codimension-two unfoldings of homoclinic flip bifurcations are presented. Then we show that the orbit flip and inclination flip both feature the creation and destruction of a cusp horseshoe. Furthermore, we show near which resonant flip bifurcations a homoclinic-doubling cascade occurs.

This allows us to glue the respective codimension-two unfoldings of homoclinic flip bifurcations together on a sphere around the central singularity. The so obtained three-parameter unfoldings are still conjectural in part, but constitute the simplest, consistent glueings.

Keywords: homoclinic bifurcation, inclination flip, orbit flip, homoclinic-doubling cascade, cusp horseshoe

1 Introduction

Consider a smooth family of vector fields $\{X_\mu\}$ on $\mathbf{R}^3$, where $\mu = (\mu_1, \mu_2, \mu_3) \in \mathbf{R}^3$. By changing coordinates if necessary, we arrange that the origin of the phase space is an equilibrium, independently of μ. We restrict our attention to the situation that $DX_\mu(\mathbf{0})$ has three distinct real eigenvalues, and without loss of generality we assume that the stable manifold $W^{ss,s}(\mathbf{0})$ is two dimensional. Let λ_{ss}, λ_s and λ_u be the eigenvalues of $DX_\mu(\mathbf{0})$, which we define by $\lambda_{ss} < \lambda_s < 0 < \lambda_u$. (For notational convenience we often do not indicate dependence on μ.) For later reference, we define the ratios $\alpha = -\lambda_{ss}/\lambda_u$ and $\beta = -\lambda_s/\lambda_u$ of the eigenvalues, which will turn out to be important parameters. (In fact one can scale $\{X_\mu\}$ to achieve that $\lambda_u = 1$ independently of μ.)

Suppose now that Γ_μ is a homoclinic orbit of X_μ. Then Γ_μ is of codimension-one if

(G1) $\lambda_s + \lambda_u \neq 0$,

(G2) $\Gamma_\mu \not\subset W^{ss}(\mathbf{0})$, and

(G3) $W^{s,u}(\mathbf{0})$ intersects $W^{ss,s}(\mathbf{0})$ transversally along Γ_μ.

Here $W^{ss}(\mathbf{0})$ denotes the one-dimensional strong-stable manifold of $\mathbf{0}$, and $W^{s,u}(\mathbf{0})$ is a two dimensional center-unstable manifold of $\mathbf{0}$; see also [Hom96]. Condition (G1) is a non-resonance condition, and (G2) means that Γ_μ must be tangent to the weak stable direction. Condition (G3) requires that the stable manifold $W^{ss,s}(\mathbf{0})$, if followed along Γ_μ, returns along the strong stable direction $W^{ss}(\mathbf{0})$. Consequently, there are two possible cases: the resulting surface may be a (topological) cylinder or a Möbius strip, that is, it is either orientable or twisted.

If (G1) is still satisfied, but (G2) or (G3) are not then (under extra genericity conditions) Γ_μ is a codimension-two homoclinic orbit. If only (G2) is not satisfied then Γ_μ is called an *orbit flip homoclinic orbit*, meaning that the homoclinic orbit is formed by the strong stable manifold $W^{ss}(\mathbf{0})$; see Figure 1. If only (G3) is not satisfied then Γ_μ is called an *inclination flip homoclinic orbit*, and the stable manifold $W^{ss,s}(\mathbf{0})$, if followed along Γ_μ, returns along the weak stable direction $W^s(\mathbf{0})$ as illustrated in Figure 2.

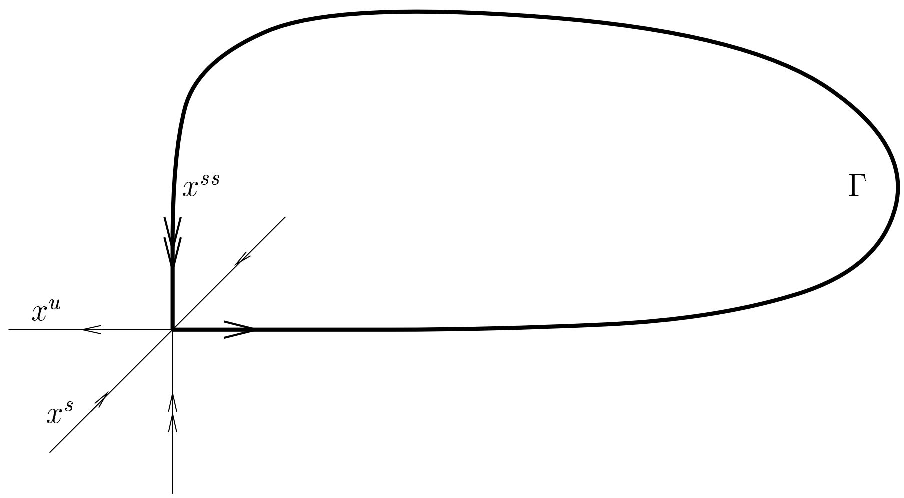

Figure 1: The orbit flip.

Recently, much progress has been made in finding the codimension-two unfoldings of the homoclinic flip bifurcations; see [KKO93a, KKO93b, HKK94, KKO96, Nau96a, Nau96b, Nii96, San93]. (The orientation of $W^{ss,s}(\mathbf{0})$ changes in both cases, hence, the name flip bifurcations.) It is an interesting fact that the orbit flip and the inclination flip lead to much the same unfoldings. There are essentially three different possibilities: **A** no extra bifurcations, **B** homoclinic-doubling (the appearance of a curve of two-homoclinic orbits that pass very close to the equilibrium once before closing), and **C** a very complicated bifurcation structure that includes n-homoclinic orbits of any period n, as well as shift-dynamics through the creation and destruction of a cusp horseshoe; see Section 2 and Figure 5. Which case occurs depends on the ratios α and β as shown in Figure 4.

In this paper we present three-parameter unfoldings of a codimension-three resonant homoclinic flip orbit Γ that exists for $\mu = 0$ in the smooth family X_μ of vector fields. We consider all resonant orbit flip and resonant inclination flip bifurcations, given by choosing (α, β) from one of the

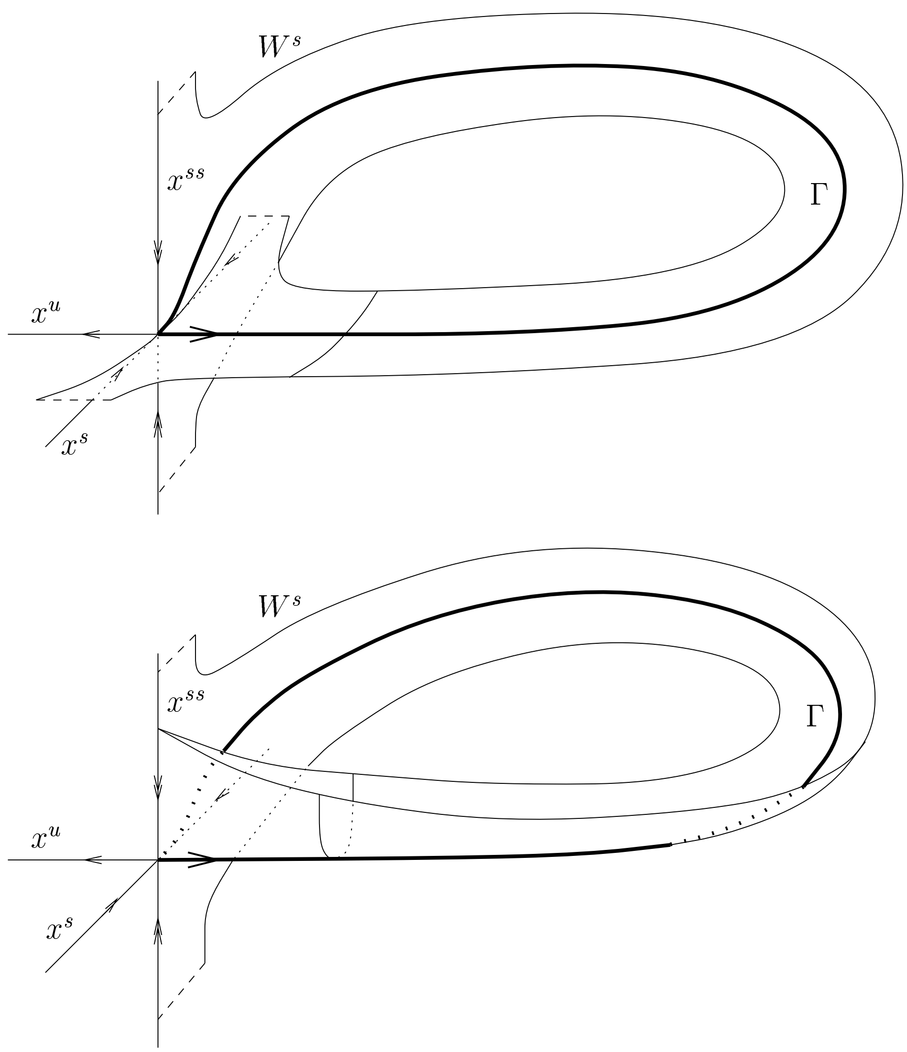

Figure 2: The two cases of the inclination flip for $\alpha < 2\beta$ (top) and $\alpha > 2\beta$ (bottom).

boundary curves in Figure 4. (Note that there are other codimension-three situations which we do not discuss here, for example, the orbit/inclination flip homoclinic orbit, the weak inclination flip and the weak orbit flip; see Section 2 and [Nau96a].) Apart from being the next logical step in studying homoclinic bifurcations, our motivation was the proof of existence of a cascade of homoclinic-doubling bifurcations in [HKN97], where a homoclinic orbit undergoes successive homoclinic-doublings. Such a cascade can be found near resonant homoclinic flip orbits; see Section 3. The following questions arise: What does the codimension-three unfolding of such resonant homoclinic flip bifurcations look likeΓ What role does the homoclinic-doubling cascade play in itΓ

In our study we adopt the topological point of view of glueing corresponding codimension-two unfoldings to each other. This idea has been very useful in the analysis of codimension-three unfoldings of degenerate equilibria of vector fields; examples are [DRS91, KR96]. Imagine a sphere around the origin in μ-space, for which there is a codimension-three homoclinic orbit Γ. Suppose that for $(\mu_1, \mu_2) = (0, 0)$ and $\mu_3 \neq 0$ there is a codimension-two homoclinic orbit Γ_{μ_3}, whose two codimension-two unfoldings near $(\mu_1, \mu_2) = (0, 0)$ for $\mu_3 > 0$ and for $\mu_3 < 0$ are known. The task is now to glue these two codimension-two unfoldings to each other on the surface of the sphere. In other words, the question is to find the additional bifurcations, away from $(\mu_1, \mu_2) = (0, 0)$ that are necessary to get a consistent bifurcation diagram. Under the assumption that the bifurcation set, or at least the parts of it that we are interested in, has conic structure near $\mu = 0$, the bifurcations on the sphere represent the codimension-three unfolding.

We present bifurcation diagrams for the three existing transitions, namely for

- the transition from **A** to **B**,
- the transition from **B** to **C** involving a homoclinic-doubling cascade, and
- the transition from **B** to **C** without a homoclinic-doubling cascade, but with an inclination flip of type **C** instead.

Figures 9 through 15 show the different unfoldings of codimension-three homoclinic orbits; see Section 4 for an explanation. Although still conjectural, they constitute the simplest, consistent glueings that take into account all known information on codimension-two homoclinic bifurcations and on the homoclinic-doubling cascade. Resonant homoclinic flip bifurcations were independently considered by J. Sotomayor, and the case of the transition from **A** to **B** is treated by his student M. Montealegre in [Mon96].

Codimension-two flip bifurcations have been found in several applications, for example in [Ko95, ZN98], and they can be detected and followed in parameter space with the package AUTO/HomCont [DCFKSW97]. By monitoring the eigenvalues resonant flip bifurcations can be detected in applications quite easily. There is also the model system due to Sandstede [San97] in which resonant flip bifurcations can be studied. However, it is quite difficult to check numerically that the bifurcation diagrams we presented are correct, because at present there is no method that allows homoclinic branch switching from a curve of homoclinic n-orbits to a curve of homoclinic $2n$-orbits. Developing such a method is in progress with the goal of numerically continueing homoclinic-doubling cascades in the unfoldings presented here. Furthermore, this will allow one to investigate quantitative features near resonant flip bifurcations in models from applications.

This paper is organized as follows. In Section 2 we summarize what is known about the unfoldings of codimension-two homoclinic orbits. We also give a treatment of the existence and destruction of cusp horseshoes. In order not to interrupt the main line of the paper, we put much of this material in Appendix A. The homoclinic-doubling cascade is discussed in Section 3. The bifurcation diagrams of the codimension-three bifurcations are derived and presented in Section 4. A second appendix, Appendix B, contains an exposition of asymptotic expansions for local transition maps, which play a fundamental role in the computations.

2 Codimension-two unfoldings

In this section we summarize known results on codimension-two homoclinic bifurcations. Recall from the introduction that bifurcation diagrams of homoclinic flip bifurcations come in three different cases, which we labeled **A**, **B** and **C**. Case **A** shows no additional bifurcations, case **B** is the homoclinic doubling bifurcation and case **C** involves n-homoclinic orbits for all integers n. Which case occurs depends on eigenvalue conditions. For homoclinic flip bifurcations in case **C**, only partial bifurcation diagrams were known. We

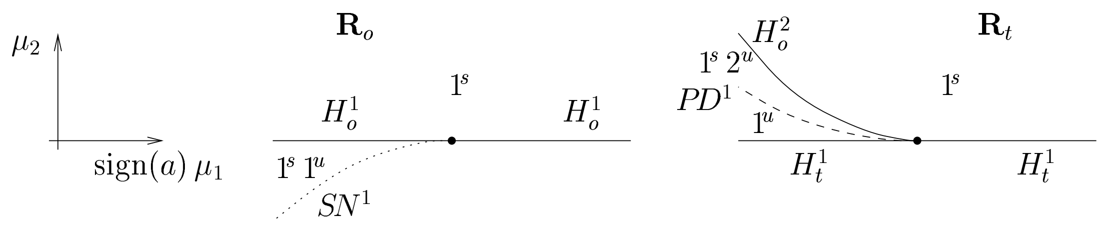

Figure 3: The different cases of unfoldings for the resonant homoclinic bifurcation. Note that a is the constant in the normal form of the return map.

extend the known results for this case and provide complete bifurcation diagrams, as far as homoclinic bifurcations are concerned. In particular, we prove the existence of cusp horseshoes and analyse their annihilation.

Consider a smooth two parameter family $\{X_\mu\}$, $\mu = (\mu_1, \mu_2) \in \mathbf{R}^2$, of vector fields on $\mathbf{R}^3$ possessing a hyperbolic singularity in the origin $\mathbf{0}$, such that $DX_\mu(\mathbf{0})$ has three distinct real eigenvalues λ_{ss}, λ_s and λ_u with $\lambda_{ss} < \lambda_s < 0 < \lambda_u$. At $\mu = 0$, X_μ possesses a homoclinic orbit Γ. Take coordinates (x_{ss}, x_s, x_u) so that

$$DX_\mu(\mathbf{0}) = \lambda_{ss} x_{ss} \frac{\partial}{\partial x_{ss}} + \lambda_s x_s \frac{\partial}{\partial x_s} + \lambda_u x_u \frac{\partial}{\partial x_u} \qquad (1)$$

and recall that $\alpha = -\lambda_{ss}/\lambda_u$ and $\beta = -\lambda_s/\lambda_u$.

2.1 Homoclinic orbit at resonance

Suppose the homoclinic orbit Γ of X_0 is a homoclinic orbit at resonance, that is, that (G1) is not satisfied. This bifurcation was treated in [CDF90]; see also [KKO93a, San93]. Natural parameters to study an unfolding of the homoclinic orbit at resonance are $\mu_1 = \beta - 1$ and μ_2 being the signed distance between stable and unstable manifolds, in a cross section. That is, for some small δ and in local coordinates in which the local stable manifold is given by $\{x_u = 0\}$, we define μ_2 by $W^u(\mathbf{0}) \cap \{x_s = \delta\} = (*, \delta, \mu_2)$. Observe that the primary homoclinic orbit exists for $\mu_2 = 0$. Assuming an additional nondegeneracy condition [CDF90], there are two different bifurcation diagrams,

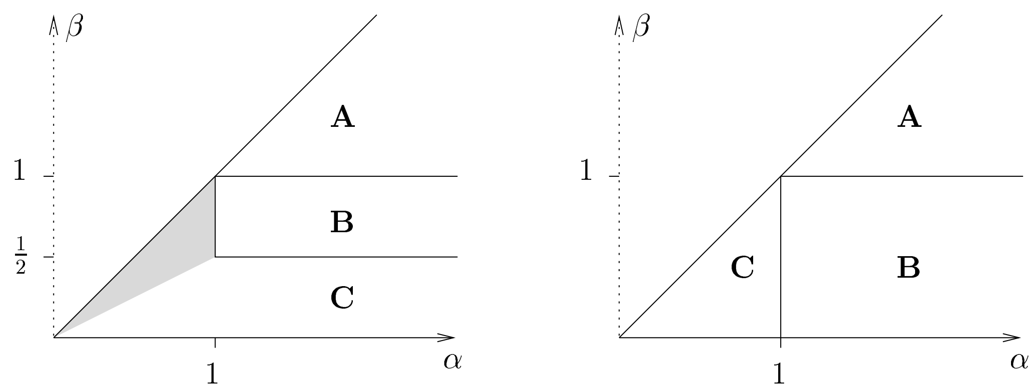

Figure 4: The regions in the (α, β)-plane of different unfoldings **A**, **B** and **C** for the orbit flip (right) and for the inclination flip (left). The shaded and the unshaded region of **C** on the left differ by the the topology of W^u at the inclination flip as shown in Figure 2.

depending on whether the homoclinic orbit at $(\mu_1, \mu_2) = (0, 0)$ is orientable or twisted. The bifurcation diagrams are given in Figure 3.

2.2 Flip homoclinic orbit

Suppose Γ is a flip homoclinic orbit. Then in the unfolding the primary homoclinic orbit switches from orientable to twisted.

Different bifurcation diagrams exist, depending on the values of α and β as depicted in Figure 4. All cases of codimension-two bifurcation diagrams near $\mu = (\mu_1, \mu_2) = (0, 0)$ can be found in Figure 5.

case A (orbit or inclination flip: $\alpha > \beta > 1$):
This case is easily studied using the fact that the Poincaré return map on a cross section is an expansion. Indeed, it is immediate from this fact that at most one 1-periodic orbit can exist.

case B (orbit flip:$\alpha > 1$, $\beta < 1$, inclination flip $\alpha > 1$, $1/2 < \beta < 1$):
This bifurcation is called a homoclinic-doubling bifurcation. The existence of the depicted bifurcation curves was established for the orbit flip in [San93] and for the inclination flip in [KKO93a, KKO93b, HKN97].

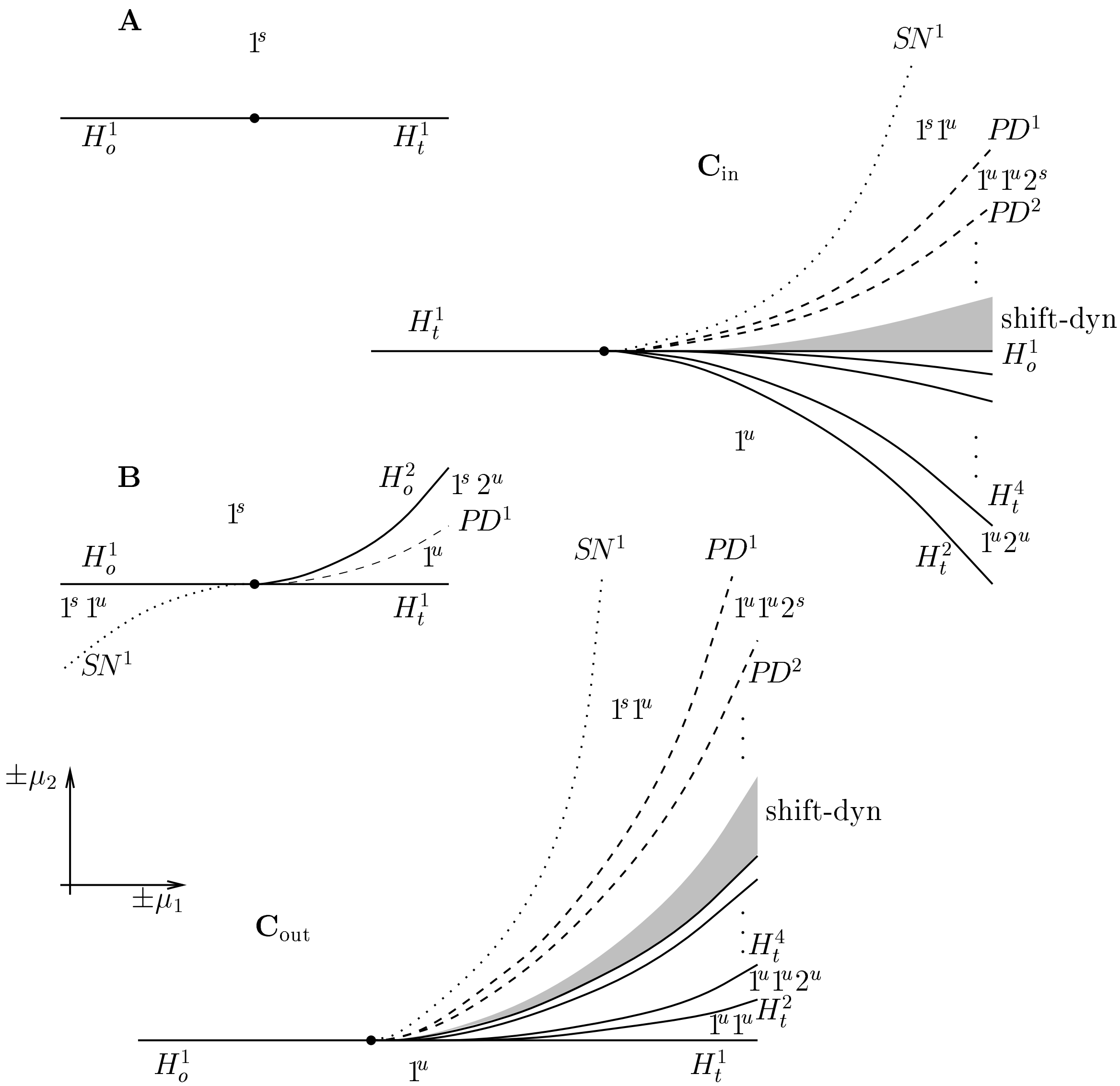

Figure 5: The different cases of unfoldings for the inclination flip and the orbit flip. In **A** no extra bifurcations occur, and **B** is the hclinic-doudoubling. The most complicated case **C** comes in the two variations $\mathbf{C}_{\text{in}}$ and $\mathbf{C}_{\text{out}}$, depending on how the horseshoe is formed. Stable and unstable periodic orbits of different periods are shown.

case C (orbit flip: $\beta < \alpha < 1$, inclination flip $\alpha < 1$ or $\beta < 1/2$): There are two cases $\mathbf{C}_{\text{in}}$ and $\mathbf{C}_{\text{out}}$. Partial bifurcation diagrams have been obtained in [San93] for the orbit flip, and in [Nau96a] for the inclination flip in the region defined by $\alpha < 1$ or $\beta < \frac{1}{2}$. In particular, these references give the existence of curves of n-homoclinic orbits, for each integer n, in the unfolding. In [HKK94] partial bifurcation diagrams have been obtained in the region $\alpha > 2\beta$ and $\beta < \frac{1}{2}$, under the additional assumption that the vector field near $\mathbf{0}$ is smoothly linearizable. As far as homoclinic bifurcations are concerned, the bifurcation diagrams in [HKK94] are complete. We remark that Hénon type strange attractors can be expected to occur in the unfolding, see [Nau96b, Nau98].

We now discuss the orbit flip and the inclination flip separately for (α, β) from region **C**. We introduce natural parameters and study the existence and bifurcations of cusp horseshoes. Certain nondegeneracy conditions must be assumed in the bifurcation study, as we will make clear. Our arguments will show that two different cases exist, an inward twist case and an outward twist case. This corresponds to the two bifurcation diagrams $\mathbf{C}_{\text{in}}$ and $\mathbf{C}_{\text{out}}$ in Figure 5. In fact, we provide a complete picture of the homoclinic bifurcations that occur in the unfolding, both for the orbit flip and the two types of inclination flips and thus extend the known results. In our analysis we use no linearizability assumptions.

2.3 Orbit flip

For some small δ, let Σ^{in}, Σ^{out} be the cross-sections

$$\begin{aligned} \Sigma^{in} &= \{x_{ss} = \delta, |x_s|, |x_u| \leq |\delta|\}, \\ \Sigma^{out} &= \{x_u = \delta, |x_{ss}|, |x_s| \leq |\delta|\}. \end{aligned}$$

We may assume that they both intersect the homoclinic orbit Γ of X_0. By a linear rescaling we may assume that $\delta = 1$. Take coordinates (x_s, x_u) on Σ^{out} and (x_{ss}, x_s) on Σ^{in} obtained by restriction of the coordinates (x_{ss}, x_s, x_u) near the origin. Let $\Phi_{loc} : \Sigma^{in} \mapsto \Sigma^{out}$ be the local transition map and let $\Phi_{far} : \Sigma^{out} \to \Sigma^{in}$ be the global transition map. The Poincaré return map Φ on Σ^{in} is the composition $\Phi = \Phi_{loc} \circ \Phi_{far}$. Observe that Φ_{far} is a local diffeomorphism. In Appendix B, asymptotic expansions for Φ_{loc} are given, valid after a smooth change of coordinates; see Proposition B.5. Using these expansions, we can write Φ as

$$\Phi(x_s, x_u) = \begin{pmatrix} \mu_1 + Ax_u^\alpha + Bx_s x_u^\beta + \mathcal{O}(x_u^{\alpha+\omega} + x_s^2 x_u^\beta + |x_s| x_u^{\beta+\omega}) \\ \mu_2 + Cx_u^\alpha + Dx_s x_u^\beta + \mathcal{O}(x_u^{\alpha+\omega} + x_s^2 x_u^\beta + |x_s| x_u^{\beta+\omega}) \end{pmatrix}, \tag{2}$$

for some $\omega > 0$. This also identifies the two parameters μ_1 and μ_2: $(\mu_1, \mu_2) = \Phi(0,0)$ are the coordinates of the first intersection of $W^u(\mathbf{0})$ with Σ^{in}.

We assume that $C \neq 0$; the case $C = 0$ corresponds to an inclination flip. We also assume $D \neq 0$. The degenerate case $D = 0$ is called a weak orbit flip [Nau96a]. Let us give an equivalent formulation of this last non-degeneracy condition. At the bifurcation point $(\mu_1, \mu_2) = (0,0)$, the image $\Phi_{far}^{-1}(W^{ss,s}(\mathbf{0}) \cap \Sigma^{out})$ is the graph of a map

$$t \mapsto (at + \mathcal{O}(t^2), t).$$

Then $a \neq 0$ precisely if $D \neq 0$.

We now show that Φ possesses horseshoes for parameter values (μ_1, μ_2) from a wedge, indicated in Figure 5 as a shaded region. The size of these horseshoes shrinks to 0 as $\mu_1 \to 0$. A suitable rescaling brings these horseshoes to unit size, which fascilitates a study of their properties and bifurcations. We will now give the proper rescaling and indicate how this enables a study of the horseshoes. Let rescaled coordinates $(\bar{x}_s, \bar{x}_u)$ be given by

$$\begin{aligned} x_s &= \mu_1 + |\mu_1|^\nu \bar{x}_s, \\ x_u &= |\mu_1|^\sigma \bar{x}_u, \end{aligned}$$

where $\sigma = 1/(\alpha - \beta)$ and $\nu = \alpha/(\alpha - \beta)$. A computation yields the following result.

Proposition 2.1 *Let $\bar{\Phi}$ be the Poincaré return map in the rescaled coordinates $(\bar{x}_s, \bar{x}_u)$. Write $s = \mu_2 |\mu_1|^{-\alpha/(\alpha-\beta)}$. Then, for some $\omega > 0$,*

$$\bar{\Phi}(\bar{x}_s, \bar{x}_u) = \begin{pmatrix} A\bar{x}_u^\alpha + B\bar{x}_u^\beta + \mathcal{O}(|\mu_1|^\omega \bar{x}_u^\beta) \\ |\mu_1|^{\frac{\alpha-1}{\alpha-\beta}} \left(s + C\bar{x}_u^\alpha + Dsign(\mu_1)\bar{x}_u^\beta + \mathcal{O}(|\mu_1|^\omega \bar{x}_u^\beta)\right) \end{pmatrix}.$$

This proposition shows that the rescaled Poincaré return map $\bar{\Phi}$ is close to a one-dimensional map, if we take (μ_1, μ_2) near 0 from a region in which $s = \mu_2|\mu_1|^{-\alpha/(\alpha-\beta)}$ is bounded. As $\mu_1 \to 0$, taking $(\bar{x}_s, \bar{x}_u)$ from some compact box $[-l, l] \times [0, k]$, $\bar{\Phi}$ converges to the one-dimensional map

$$\bar{x}_u \quad \mapsto \quad \begin{pmatrix} A\bar{x}_u^\alpha + B\bar{x}_u^\beta \\ |\mu_1|^{\frac{\alpha-1}{\alpha-\beta}} g(\bar{x}_u) \end{pmatrix}, \tag{3}$$

where

$$g(\bar{x}_u) \quad = \quad s + C\bar{x}_u^\alpha + D\mathrm{sign}(\mu_1)\bar{x}_u^\beta.$$

If $\mu_1 D$ and C have opposite sign, then $\bar{x}_u \mapsto |\mu_1|^{(\alpha-1)/(\alpha-\beta)} g(\bar{x}_u)$ is unimodal and has a graph as depicted in Figure 8. If the one-dimensional map (3) possesses a hyperbolic horseshoe, then also Φ does for μ_1 small enough and of the correct sign. An easy analysis yields the existence of an interval of values of s, such that $\bar{x}_u \mapsto |\mu_1|^{(\alpha-1)/(\alpha-\beta)} g(\bar{x}_u)$ maps two disjoint subintervals of $[0, k]$ onto $[0, k]$, with slope larger then 1 (for suitable large enough k and l). For such values of s and μ_1 (corresponding to a wedge shaped region in the (μ_1, μ_2) parameter plane), the one-dimensional map (3) has a hyperbolic horseshoe.

The reason for the appearance of two different cases, an inward twist case and an outward twist case, follows from a geometric observation. A box $\{0 < \bar{x}_u \leq k, |\bar{x}_s| \leq l\}$ in the rescaled coordinates, corresponds to a small box D_{μ_1} in the original coordinates, adjacent to the local stable manifold in Σ^{in}. The image $\Phi_{far}^{-1}(D_{\mu_1})$ is on one side of the intersection of $W^{ss,s}(\mathbf{0})$ with Σ^{out}, which yields the two different cases. In Figure 6 one case is indicated, where the horseshoe exists if $\mu_2 = 0$ (note that the horseshoe is depicted in Σ^{out}). This case we call the inward twist case $\mathbf{C}_{\mathrm{in}}$. It is clear that Φ, restricted to D_{μ_1}, does not possess a horseshoe if the image $\Phi_{far}^{-1}(D_{\mu_1})$ lies on the other side of $W^{ss,s}(\mathbf{0}) \cap \Sigma^{out}$, at $\mu_2 = 0$. However, by varying the value of μ_2, a horseshoe will be created. This case is called the outward twist case $\mathbf{C}_{\mathrm{out}}$. Which case occurs can be read off from the sign of C in (2): $C > 0$ corresponds to the outward twist case, whereas $C < 0$ corresponds to the inward twist case. The inward and outward twist cases lead to different one-dimensional maps: for the inward twist case, the one-dimensional map g is unimodal with a maximum, whereas for the outward twist case it is unimodal with a minimum, see Figure 8.

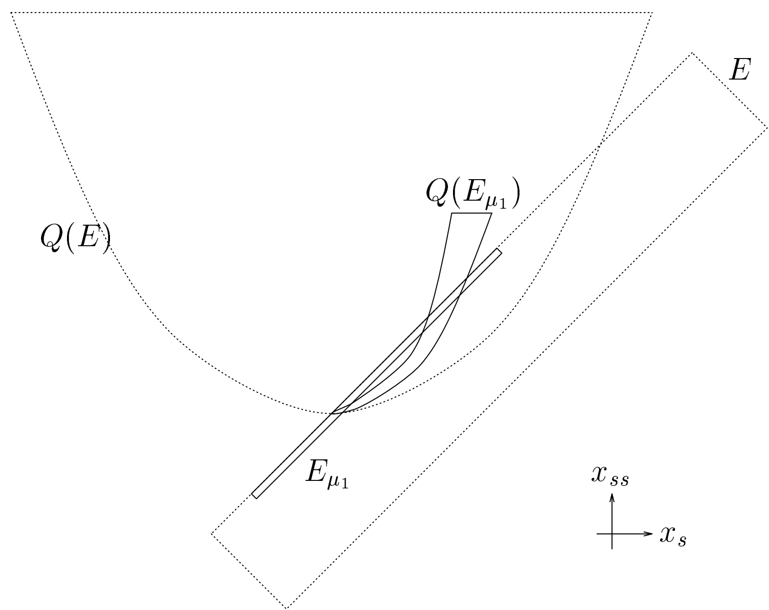

Figure 6: Depicted is the shape of the cusp horseshoe as it occurs in the unfolding of an orbit flip, lying in the cross section Σ^{out}. A small subdomain E_{μ_1} of the domain E of the return map Q on Σ^{out}, is mapped by Q into a horseshoe shape over itself.

Analysis of the rescaled return map $\bar{\Phi}$ enables a characterization of the sequence of homoclinic bifurcations in which the horseshoe annihilates. Varying s, one encounters interval maps as in Figure 8, that do not possess a full horseshoe, since there are no two subintervals that are mapped onto the whole interval. An analysis of such interval maps explains the sequences of bifurcations in which the horseshoe is destructed, see [HKK94, Hom96]. The rescaled return map $\bar{\Phi}$ has the same bifurcation structure as the one-dimensional map (3) as far as the homoclinic bifurcations are concerned. Appendix A contains information on this annihilation process of the horseshoe and the ensueing combinatorics of periodic orbits.

2.4 Inclination flip

For the inclination flip, we follow the same program as for the orbit flip. We will be briefer than in the previous subsection, and mainly pay attention to reductions to one-dimensional maps. The rest of the arguments can be filled in by following the reasoning for the orbit flip.

For some small δ, let Σ^{in}, Σ^{out} be the cross-sections

$$\begin{aligned}\Sigma^{in} &= \{x_s = \delta, |x_{ss}|, |x_u| \leq |\delta|\},\\ \Sigma^{out} &= \{x_u = \delta, |x_{ss}|, |x_s| \leq |\delta|\},\end{aligned}$$

intersecting the homoclinic orbit Γ of X_0. By a linear rescaling we may assume that $\delta = 1$. Take coordinates (x_{ss}, x_s) on Σ^{out} and (x_{ss}, x_u) on Σ^{in} obtained by restriction of the coordinates (x_{ss}, x_s, x_u) near the origin. Let $\Phi_{loc} : \Sigma^{in} \mapsto \Sigma^{out}$ be the local transition map. Let $\Phi_{far} : \Sigma^{out} \to \Sigma^{in}$ be the global transition map, which is a local diffeomorphism. The Poincaré return map Φ on Σ^{in} is again the composition $\Phi = \Phi_{loc} \circ \Phi_{far}$.

The case $\alpha = 2\beta$ is degenerate, and we assume that $\alpha - 2\beta \neq 0$. The two cases with different sign of $\alpha - 2\beta$ are treated separately; see also Figure 2.

The case $\alpha > 2\beta$, $\beta < 1/2$.

Proposition B.2 in Appendix B provides asymptotic expansions for the local transition map Φ_{loc}. Because Φ_{far} is a local diffeomorphism, one can write the following expression for $\Phi = \Phi_{loc} \circ \Phi_{far}$.

$$\Phi(x_{ss}, x_u) = \begin{pmatrix} p + Bx_u^{\beta} + \mathcal{O}(x_u^{\beta+\omega}) \\ \mu_2 + \mu_1 x_u^{\beta} + Dx_u^{2\beta} + \mathcal{O}(|\mu_1| x_u^{\beta+\omega} + x_u^{2\beta+\omega}) \end{pmatrix}, \qquad (4)$$

for some $\omega > 0$. This also identifies the parameters (μ_1, μ_2). For generic families the constant D is nonzero at $(\mu_1, \mu_2) = (0, 0)$, which we assume to be the case.

As above we will use a rescaling to study the existence of hyperbolic horseshoes. Consider rescaled coordinates $(\bar{x}_{ss}, \bar{x}_u)$ given by

$$\begin{aligned} x_u &= |\mu_1|^{\sigma} \bar{x}_u,\\ x_{ss} - p &= \bar{x}_{ss}, \end{aligned}$$

where $\sigma = 1/\beta$.

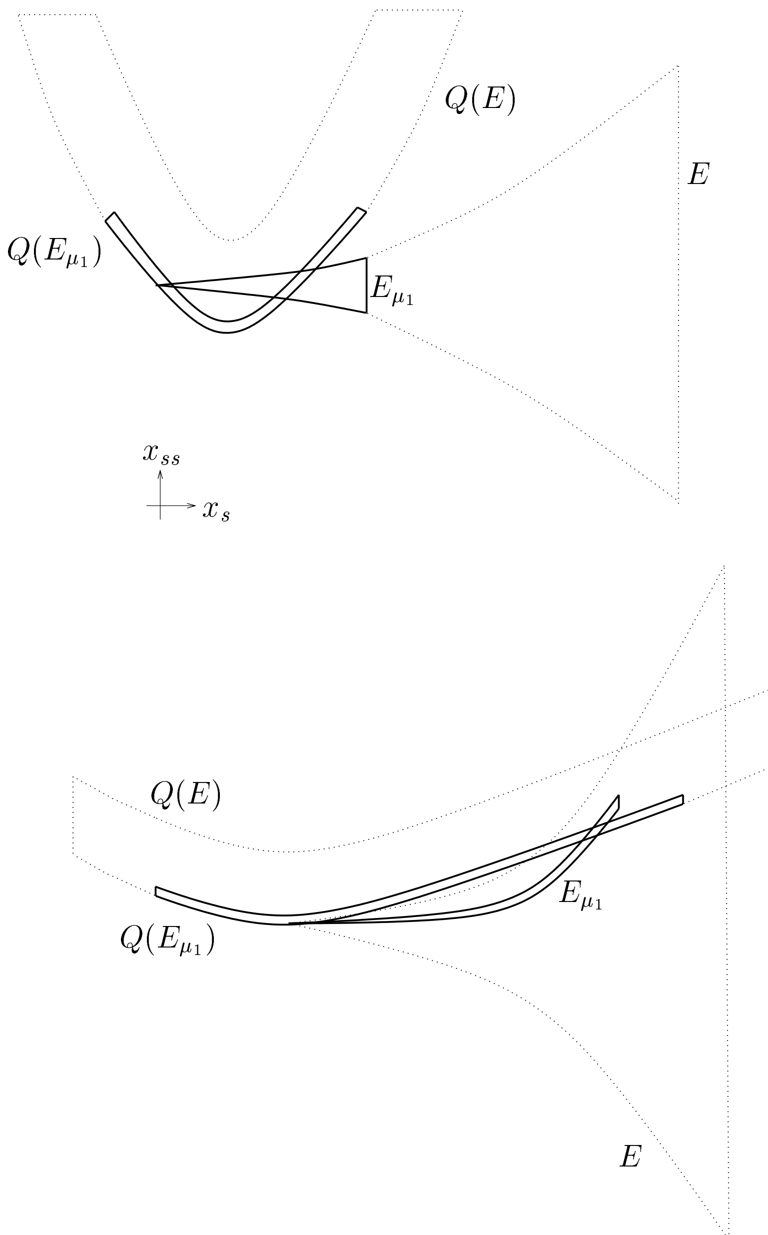

Figure 7: Cusp horseshoes in the unfolding of the inclination flip. The top picture is for $\alpha > 2\beta$ and $0 < \beta < 1/2$ and shows the inward twist $\mathbf{C}_{\rm in}$. The bottom picture is for $\alpha < 2\beta$ and $\alpha < 1$ and shows the outward twist $\mathbf{C}_{\rm out}$. In both cases a small subdomain E_{μ_1} of the domain E of the return map Q on Σ^{out}, is mapped by Q into a horseshoe shape over itself.

Proposition 2.2 *Let $\bar{\Phi}$ be the Poincaré return map in the rescaled coordinates $(\bar{x}_s, \bar{x}_u)$. Write $s = \mu_2 |\mu_1|^{-2}$. Then, for some $\omega > 0$,*

$$\bar{\Phi}(\bar{x}_{ss}, \bar{x}_u) = \begin{pmatrix} \mathcal{O}(|\mu_1|^{\omega} \bar{x}_u^{\beta}) \\ |\mu_1|^{2-\frac{1}{\beta}} \left(s + sign(\mu_1)\bar{x}_u^{\beta} + D\bar{x}_u^{2\beta} + \mathcal{O}(|\mu_1|^{\omega}\bar{x}_u^{\beta})\right) \end{pmatrix}.$$

As $\mu_1 \to 0$, restricting $\bar{x}_u$ to a compact interval and parameters (μ_1, μ_2) to a region in which s is bounded, $\bar{\Phi}$ converges to the one-dimensional map

$$\bar{x}_u \mapsto \begin{pmatrix} 0 \\ |\mu_1|^{2-1/\beta} \left(s + \mathrm{sign}(\mu_1)\bar{x}_u^{\beta} + D\bar{x}_u^{2\beta}\right) \end{pmatrix}.$$

This map is analysed as before. Figure 7 (top) gives an idea of the geometry of the horseshoe. Note that the inward case is depicted, where the horseshoe exists if $\mu_2 = 0$.

The case $\alpha < 2\beta$, $\alpha < 1$.

Applying Proposition B.2 from Appendix B, we can write

$$\Phi(x_{ss}, x_u) = \begin{pmatrix} p + Ax_u^{\alpha} + Bx_u^{\beta} + \mathcal{O}(x_u^{\alpha+\omega}) \\ \mu_2 + Cx_u^{\alpha} + \mu_1 x_u^{\beta} + \mathcal{O}(x_u^{\alpha+\omega}) \end{pmatrix}, \tag{5}$$

for some $\omega > 0$. We assume $p \neq 0$; the case $p = 0$ is called a weak inclination flip [Nau96a].

Consider rescaled coordinates $(\bar{x}_{ss}, \bar{x}_u)$ given by

$$\begin{aligned} x_u &= |\mu_1|^{\sigma} \bar{x}_u, \\ x_{ss} - p &= \bar{x}_{ss}, \end{aligned}$$

where $\sigma = 1/(\alpha - \beta)$.

Proposition 2.3 *Let $\bar{\Phi}$ be the Poincaré return map in the rescaled coordinates $(\bar{x}_s, \bar{x}_u)$. Write $s = \mu_2 |\mu_1|^{-\alpha/(\alpha-\beta)}$. Then, for some $\omega > 0$,*

$$\bar{\Phi}(\bar{x}_{ss}, \bar{x}_u) = \begin{pmatrix} \mathcal{O}(|\mu_1|^{\omega} \bar{x}_u^{\beta}) \\ |\mu_1|^{\frac{\alpha-1}{\alpha-\beta}} \left(s + C(p + \bar{x}_{ss})\bar{x}_u^{\alpha} + sign(\mu_1)\bar{x}_u^{\beta} + \mathcal{O}(|\mu_1|^{\omega}\bar{x}_u^{\beta})\right) \end{pmatrix}.$$

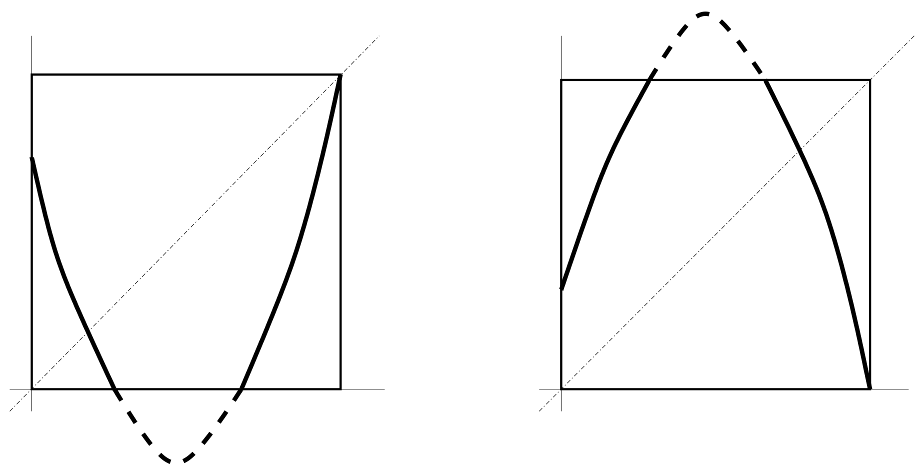

Figure 8: The one-dimensional maps occcuring in reductions of homoclinic flip bifurcations for (α, β) from region **C** are unimodal. They possess either a minimum for the outward twist case $\mathbf{C}_{\text{out}}$ (left), or a maximum for the inward twist case $\mathbf{C}_{\text{in}}$ (right).

As $\mu_1 \to 0$, the map $\bar{\Phi}$ converges to the one-dimensional map

$$\bar{x}_u \mapsto \begin{pmatrix} 0 \\ |\mu_1|^{(\alpha-1)/(\alpha-\beta)} \left(s + Cp\bar{x}_u^\alpha + \text{sign}(\mu_1)\bar{x}_u^\beta\right) \end{pmatrix}.$$

A similar analysis as before yields the existence of hyperbolic horseshoes. Figure 7 (bottom) gives an idea of the geometry of the horseshoe. Note that the outward case is depicted, where the horseshoe does not exist if $\mu_2 = 0$.

3 The homoclinic-doubling cascade

As mentioned in the introduction, one of the motivations for writing this paper, was the result in [HKN97] that near a particular orbit flip homoclinic orbit of codimension-three, cascades of homoclinic-doubling bifurcations occur. Here, a homoclinic-doubling bifurcation is a codimension-two homoclinic bifurcation with a bifurcation diagram as in case **B** in Figure 5. Pathfollow a curve of homoclinic bifurcations in the parameter plane. At a homoclinic-doubling bifurcation, continue pathfollowing the curve of doubled homoclinic orbits. A cascade of homoclinic-doubling bifurcations is present if one encounters homoclinic-doubling bifurcations μ_n in which a 2^n homoclinic orbit is created, for all positive integers n.

In [HKN97] it was established that such homoclinic-doubling cascades can occur persistently in two parameter families of vector fields. In fact, an open set of two parameter families of vector fields that contain cascades of homoclinic-doubling bifurcations is constructed. The members of the families from this open set are near a vector field with a particular resonant orbit flip homoclinic orbit:

Theorem 3.1 ([HKN97]) *Let $\{X_\mu\}$, $\mu = (\mu_1, \mu_2, \mu_3)$, be a three parameter family of vector fields unfolding an orbit flip at resonance $\alpha = 1$ with $1/2 < \beta < 1$. Suppose the number C in (2) is large enough. Let μ_1, μ_2 be defined as in Section 2.3 and let $\mu_3 = \alpha - 1$. For each μ_2 sufficiently small and positive, the two parameter family $\{Y_{\mu_1,\mu_3}\}$ given by $Y_{\mu_1,\mu_3} = X_{\mu_1,\mu_2,\mu_3}$, possesses a connected set of homoclinic bifurcation values in the (μ_1, μ_3)-parameter plane, containing a cascade (μ_1^n, μ_3^n) of homoclinic-doubling bifurcations in which a 2^n-homoclinic orbit is created. All these homoclinic-doubling bifurcations are inclination flips of type* **B**.

It is not known whether the homoclinic bifurcations in these families are unfolding generically, so that the set of homoclinic bifurcation values might be more complicated then a union of curves. For families from a residual subset of the constructed open set, homoclinic bifurcations will unfold generically.

Of basic importance in the derivation of Theorem 3.1 is the observation that a Poincaré return map on a cross section transverse to the homoclinic orbit is close to a one-dimensional map for a subset of the parameters (μ_1, μ_2, μ_3). Recall from Section 2.3 the following expression for the rescaled return map $\bar{\Phi}$.

$$\bar{\Phi}(\bar{x}_s, \bar{x}_u) = \begin{pmatrix} A\bar{x}_u^\alpha + B\bar{x}_u^\beta + \mathcal{O}(|\mu_1|^\omega \bar{x}_u^\beta) \\ |\mu_1|^{\mu_3/(\alpha-\beta)} \left(s + C\bar{x}_u^\alpha + D\mathrm{sign}(\mu_1)\bar{x}_u^\beta + \mathcal{O}(|\mu_1|^\omega \bar{x}_u^\beta)\right) \end{pmatrix},$$

for some $\omega > 0$. Here $s = \mu_2 |\mu_1|^{-\alpha/(\alpha-\beta)}$. Write $\lambda = |\mu_1|^{\mu_3/(\alpha-\beta)}$ and note that $\lambda = 1$ if $\mu_3 = 0$. Restrict parameter values to a region in which s is bounded and λ is bounded and bounded away from 0. Then $\bar{\Phi}$ is a perturbation from the one-dimensional map

$$\bar{x}_u \mapsto \begin{pmatrix} A\bar{x}_u + B\bar{x}_u^\beta \\ \lambda\left(s + C\bar{x}_u + D\mathrm{sign}(\mu_1)\bar{x}_u^\beta\right) \end{pmatrix}, \tag{6}$$

of which only the second coordinate is of importance. Observe that this reduction actually yields a family of maps, depending on the two parameters λ and s. The rescaled return map $\bar{\Phi}$ has μ_1 as a third and small parameter.

By the eigenvalue condition $1/2 < \beta < 1$, an inclination flip occuring for $\mu_3 > 0$ is a homoclinic-doubling bifurcation with a bifurcation diagram as in case **B** in Figure 5, whereas an inclination flip occuring for $\mu_3 < 0$ has the complicated bifurcation diagram depicted in case **C** in Figure 5. This remark is the background for the requirement in Theorem 3.1 that C should be sufficiently large: for C large enough all inclination flips occur for $\mu_3 > 0$, that is, for $\lambda < 1$.

The proof of Theorem 3.1 relies on a study of the above one-dimensional map, combined with a continuation theory for homoclinic orbits as developed in [HKN97]. This continuation theory is reminiscent of a similar theory developed to follow periodic orbits in [YA83], where a continuation theory for periodic orbits was used to find cascades of period-doublings.

The above reasonings can also be applied to the two different kinds of resonant inclination flips. Consider the inclination flip at the resonance $\beta = 1/2$ with $\alpha > 1$. Consider the rescaled return map $\bar{\Phi}$ from Proposition 2.2. The term $|\mu_1|^{2-1/\beta}$ in front of the second coordinate of $\bar{\Phi}$ is large for $\beta < 1/2$ and equals 1 if $\beta = 1/2$. We introduce a third parameter $\mu_3 = \beta - \frac{1}{2}$ and restrict to parameters for which $\lambda = |\mu_1|^{2-\frac{1}{\mu_3+1/2}}$ is bounded and bounded away from zero and $s = \mu_2|\mu_1|^{-2}$ is bounded. Then $\bar{\Phi}$, for μ_1 small, is a perturbation from the one-dimensional map

$$\bar{x}_u \mapsto \begin{pmatrix} 0 \\ \lambda\left(s + \mathrm{sign}(\mu_1)\sqrt{\bar{x}_u} + D\bar{x}_u\right) \end{pmatrix}, \tag{7}$$

which depends on the two parameters λ and s.

Applying arguments developed in [HKN97] allows to show the existence of homoclinic-doubling cascades in the unfolding of this resonant inclination flip. Indeed, as mentioned above, the proof of Theorem 3.1 relies on a study of the one-dimensional map obtained from rescaling a Poincaré return map, plus an application of a continuation theory for homoclinic orbits. Since the one-dimensional map for the resonant inclination flip is similar to the one obtained for the resonant orbit flip, the reasoning in [HKN97] goes through, and we obtain the following result.

Theorem 3.2 *Let $\{X_\mu\}$, $\mu = (\mu_1, \mu_2, \mu_3)$, be a three parameter family of vector fields unfolding an inclination flip at resonance $\beta = \frac{1}{2}$ with $\alpha > 1$. Let μ_1, μ_2 be defined as in Section 2.4 and let $\mu_3 = \beta - \frac{1}{2}$. Suppose the number D in (4) is large enough. For each μ_2 sufficiently small and positive, the two parameter family $\{Y_{\mu_1,\mu_3}\}$ given by $Y_{\mu_1,\mu_3} = X_{\mu_1,\mu_2,\mu_3}$, possesses a connected set of homoclinic bifurcation values in the (μ_1, μ_3)-parameter plane, containing a cascade (μ_1^n, μ_3^n) of homoclinic-doubling bifurcations in which a 2^n-homoclinic orbit is created. All these homoclinic-doubling bifurcations are inclination flips of type* **B**.

In one respect the homoclinic-doubling cascades in the unfolding of this resonant inclination flip differ from those occuring in the unfolding of the resonant orbit flip. Namely, in the limit $\mu_1 = 0$ the rescaled return map becomes the one-dimensional map (7), which does not possess homoclinic-doubling cascades. We expect homoclinic-doubling bifurcations in a cascade to occur very close to eachother if μ_1 is small; compare the discussion in [HKN97] and in Section 4.4.

The inclination flip at the resonance $\alpha = 1$ with $1/2 < \beta < 1$ can be treated in the same way. The rescaled return map $\bar{\Phi}$, for μ_1 small, is a perturbation from the one-dimensional map

$$\bar{x}_u \mapsto \begin{pmatrix} 0 \\ \lambda\left(s + Cp\bar{x}_u + \mathrm{sign}(\mu_1)\bar{x}_u^\beta\right) \end{pmatrix}, \tag{8}$$

where $\lambda = |\mu_1|^{\frac{\alpha-1}{\alpha-\beta}}$ and $s = \mu_2|\mu_1|^{\frac{-\alpha}{\alpha-\beta}}$.

Theorem 3.3 *Let $\{X_\mu\}$, $\mu = (\mu_1, \mu_2, \mu_3)$, be a three parameter family of vector fields unfolding an inclination flip at resonance $\alpha = 1$ with $1/2 < \beta < 1$. Suppose the number Cp in (5) is large enough. Let μ_1, μ_2 be defined as in Section 2.4 and let $\mu_3 = \alpha - 1$. For each μ_2 sufficiently small and positive, the two parameter family $\{Y_{\mu_1,\mu_3}\}$ given by $Y_{\mu_1,\mu_3} = X_{\mu_1,\mu_2,\mu_3}$, possesses a connected set of homoclinic bifurcation values in the (μ_1, μ_3)-parameter plane, containing a cascade (μ_1^n, μ_3^n) of homoclinic-doubling bifurcations in which a*

2^n-homoclinic orbit is created. All these homoclinic-doubling bifurcations are inclination flips of type **B**.

4 Codimension-three unfoldings

In this section we consider the resonant flip bifurcations of codimension-three that correspond to (α, β) on the lines between the regions **A**, **B**, and **C** in Figure 4. The central singularity may be an orbit flip or an inclination flip. There are three different classes of transitions.

- The transition from **A** to **B**,
- The transition from **B** to **C** involving a homoclinic-doubling cascade. This occurs for $1/2 < \beta < 1$ and α near 1 both if the central singularity is an orbit flip or an inclination flip. This also occurs for β near $1/2$ and $\alpha > 1$ if the central singularity is an inclination flip.
- The transition from **B** to **C** without a homoclinic-doubling cascade, but with an inclination flip of type **C** instead. This occurs for $0 < \beta < 1/2$ and α near 1 if the central singularity is an orbit flip.

We take the topological point of view of glueing the respective codimension-two unfoldings from Section 2 to each other on the surface of a sphere. To this end we arrange the parameters in such a way that one codimension-two singularity sits at the north pole, and the other at the south pole. The problem is now to connect the two in a consistent way on the surface of the sphere.

In the figures we project this sphere to the plane as follows. The parameter μ_1 unfolding the twist changes sign along the vertical axis of each bifurcation diagram. Along the circle, corresponding to the bifurcating one-homoclinic orbit Γ, the parameter μ_2 (breaking Γ) changes sign. Finally, the parameter μ_3 unfolding the resonance (crossing between the respective regions **A**, **B**, and **C**) changes sign along the horizontal axis. By adjoining the point at infinity the sphere can be retrieved.

The labels of the bifurcation curves indicate the type of bifurcation. H_x^n stands for a codimension-one n-homoclinic orbit, where the subscript indicates whether the homoclinic orbit is orientable ($x = o$) or twisted ($x = t$).

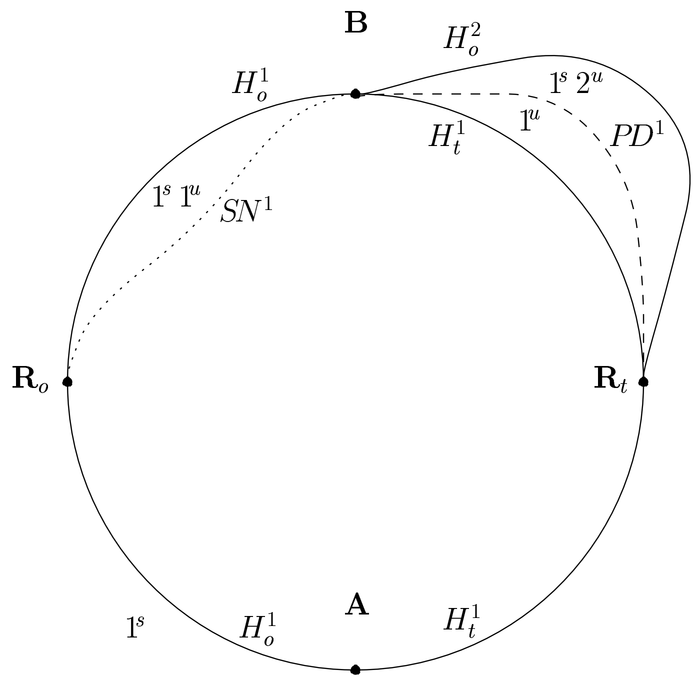

Figure 9: The transition from **A** to **B** involves the orientable and the nonorientable resonant homoclinic bifurcation.

Furthermore, PD^n denotes a period-doubling bifurcation and SN^n a saddle-node bifurcation of an n-periodic orbit. In order to show that the bifurcation diagrams are consistent we have indicated what limit cyles can be found in the different regions on each sphere. The coding n^s indicates that there is a stable n-orbit (passing n times near the origin before closing), and n^u stands for an unstable n-orbit (of saddle-type). Consequently, the limit cycles of type n^s can be found by integration or in an experiment, but those of type n^u need more advanced techniques to be detected in a given system.

4.1 Transition from A to B

We introduce the parameter $\mu_3 = 1 - \beta$, where we fix $\alpha > 1$. The central singularity may be both an orbit flip or an inclination flip. The transition from **A** to **B** when μ_3 changes sign can be resolved on the sphere if one realized that $\mu_1 = \mu_2 = 0$ defines the resonant homoclinic bifurcations from [CDF90] in Figure 3. There are the two possibilities depending on the sign of a normal form coefficient; see [CDF90]. However, on the sphere both cases are topologically as sketched in Figure 9. This case is studied in [Mon96] with the method of desingularization of families of vector fields [Rou93].

4.2 Transition from B to C involving a homoclinic-doubling cascade

This case was the main motivation for this paper because the homoclinic-doubling cascade was found in [HKN97] near a resonant orbit flip for $1/2 < \beta < 1$. In Section 3 we have seen that the homoclinic-doubling cascade is also found near a resonant inclination flip with α near 1 and $1/2 < \beta < 1$, and also near a resonant inclination flip with β near 1/2 and $\alpha > 1$. We introduce parameters (μ_1, μ_2, μ_3) as in the respective bifurcation theorems. Recall that the rescalings considered in Section 3 are defined for parameters (μ_1, μ_2, μ_3) from a region for which a function λ of the parameters is bounded and bounded away from 0 and a second function s of the parameters is bounded. This defines charts on part of the small sphere around the origin in parameter space. Small neighborhoods of the poles correspond to large and small values of λ. Near the poles the bifurcation diagram is that of the codimension-two flip bifurcations, near the northpole of case **C** and near the southpole of case **B**. It remains to study the bifurcations for parameters from the part of the sphere corresponding to large values of s. This part of the sphere is not covered by the rescalings from Section 3. A different rescaling enables a study on this part of the sphere. We discuss this for the resonant orbit flip, but similar considerations apply to the resonant inclination flips.

Let the return map $(x_s, x_u) \mapsto \Phi(x_s, x_u)$ on Σ^{in} be as in (2). Let rescaled coordinates $(\hat{x}_s, \hat{x}_u)$ be given by

$$\begin{aligned} x_s &= \mu_1 + |\mu_2|\hat{x}_s, \\ x_u &= |\mu_2|^{1/\alpha}\hat{x}_u. \end{aligned}$$

A computation yields the following result.

Proposition 4.1 *Let $\hat{\Phi}$ be the Poincaré return map in the rescaled coordinates $(\hat{x}_s, \hat{x}_u)$. Write $t = \mu_1|\mu_2|^{(\beta-\alpha)/\alpha}$ and $\nu = |\mu_2|^{(\alpha-1)/\alpha}$. Then, for some*

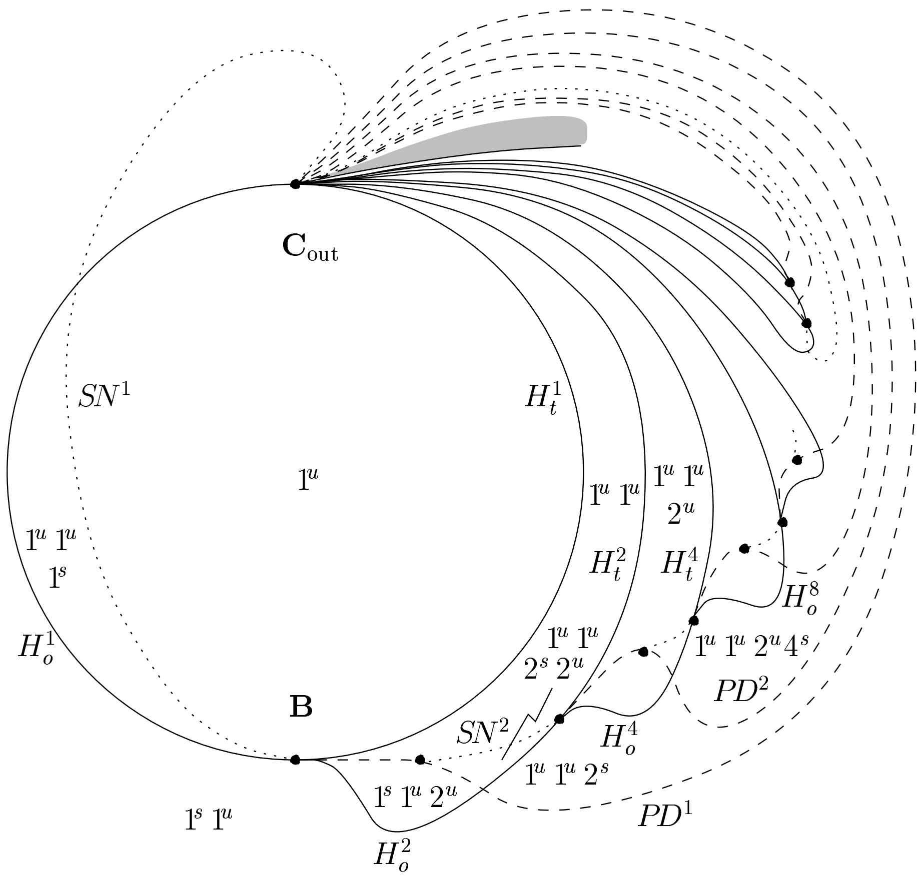

Figure 10: The transition from $\mathbf{B}$ to $\mathbf{C}_{\rm out}$ via homoclinic-doubling cascades.

$\omega > 0$,

$$\hat{\Phi}(\hat{x}_s, \hat{x}_u) = \begin{pmatrix} A\hat{x}_u^{\alpha} + Bt\hat{x}_u^{\beta} + \mathcal{O}(|\mu_2|^{\omega}\hat{x}_u^{\beta}) \\ \nu\left(sign(\mu_2) + C\hat{x}_u^{\alpha} + Dt\hat{x}_u^{\beta} + \mathcal{O}(|\mu_2|^{\omega}\hat{x}_u^{\beta})\right) \end{pmatrix}.$$

Take parameter values for which t is bounded (note that small values of t correspond to large values of s) and for which ν is bounded and bounded away from zero (small or large values of ν occur near the poles on the sphere). Then for $(\hat{x}_s, \hat{x}_u)$ from a box of the form $[-l, l] \times (0, k]$, the rescaled return

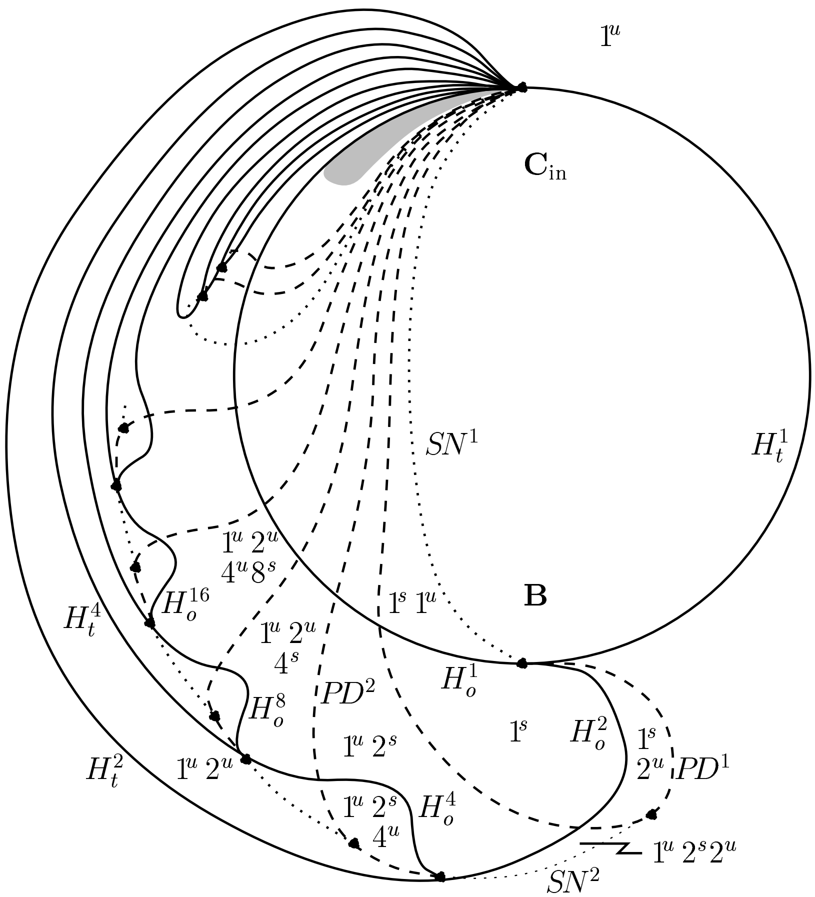

Figure 11: The transition from **B** to $\mathbf{C}_{\text{in}}$ via homoclinic-doubling cascades.

map $\hat{\Phi}$ is a perturbation from the one-dimensional map

$$\hat{x}_u \quad \mapsto \quad \begin{pmatrix} A\hat{x}_u + Bt\hat{x}_u^{\beta} \\ \nu\left(\text{sign}(\mu_2) + C\hat{x}_u + Dt\hat{x}_u^{\beta}\right) \end{pmatrix}.$$

This result plus the earlier discussions in Sections 2 and 3, show that there is a covering of the sphere by charts on which different rescalings to perturbations from one-dimensional maps exist. This enables a bifurcation study for all parameter values on the sphere. Note though that the rescalings are applied to (x_s, x_u) from a small box in Σ^{in}, whose size goes to 0 as $\mu \to 0$. Bifurcations of orbits outside this box are not captured by an analysis of the rescaled return map, compare the discussion of the codimension-two

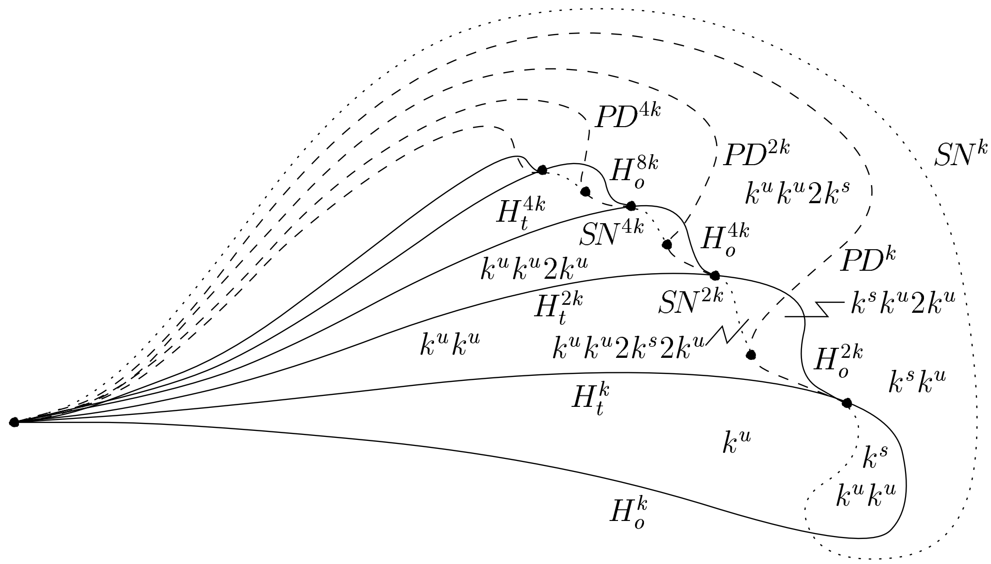

Figure 12: A k-bubble with a homoclinic-doubling cascade.

inclination flip in the appendix of [HKN97].

From a knowledge of the bifurcation structures near the poles and a study of bifurcations of the rescaled return maps from Propositions 2.1 and 4.1, on different charts of the sphere, one can draw a consistent bifurcation diagram on the sphere. The transition from **B** to **C** when μ_3 changes sign is sketched in Figures 10 and 11 for the two cases $\mathbf{C}_{\text{out}}$ and $\mathbf{C}_{\text{in}}$. These figures certainly need some interpretation. Near the codimension-two point of type **B** a period-two homoclinic orbit is born. As we follow this orbit it undergoes a cascade of homoclinic-doublings as described in Section 3. The curves of twisted homoclinic loops all end at the codimension-two point of type **C**, as do the curves of period-doublings that are associated with the homoclinic-doubling cascade. These bifurcation curves account for a part of the bifurcations that occur in the respective unfoldings of the cusp horseshoe in the cases $\mathbf{C}_{\text{out}}$ and $\mathbf{C}_{\text{in}}$. However, they account only for the bifurcations of 2^l-orbits. Therefore there are 'k-bubbles' as shown in Figure 12 that protrude from **C** into the lower half plane where $\mu_3 < 0$. (Recall that the flip bifurcations in the cascade are inclination flips, which are of type **B** only for $\mu_3 < 0$.) The fact that there is a complete cascade comes from the assumption that the respective coefficient in the expansion of the Poincaré return map is sufficiently large; see Section 3. The complete bifurcation diagram is now an infinite puzzle of k-bubbles that are organized according to the order of bifurcations near $\mathbf{C}_{\mathrm{out}}$ and $\mathbf{C}_{\mathrm{in}}$, respectively. This order is determined by the respective one-dimensional map as is explained in Appendix A; see also [HKK94].

4.3 Transition from B to C without a homoclinic-doubling cascade

This transition occurs if the central singularity is a resonant orbit flip with $0 < \beta < 1/2$. We introduce the parameter $\mu_3 = 1 - \alpha$. By looking at Figure 9 (right) it is immediately clear that there cannot be a homoclinic-doubling cascade on the sphere, because near the central singularity there are no inclination flips of type **B**. In other words, we must now make the transition from **B** to **C** with inclination flips of type **C**. This means that the point $\beta = 1/2$ is a bifurcation point for the codimension-three unfoldings we consider here. We will come back to this point of view below in Section 4.4.

The transition from **B** to **C** when μ_3 changes sign in this setting is sketched in Figures 13 and 14 for the two cases $\mathbf{C}_{\mathrm{out}}$ and $\mathbf{C}_{\mathrm{in}}$. Near the codimension-two point of type **B** a period-two homoclinic orbit is born, but now it undergoes an inclination flip bifurcation of type $\mathbf{C}_{\mathrm{in}}$. The homoclinic loop and period doubling curves all end at the codimension-two point of type **C**. They account for a part of the bifurcations that occur in the respective unfoldings of the cusp horseshoe in the cases $\mathbf{C}_{\mathrm{out}}$ and $\mathbf{C}_{\mathrm{in}}$. There are 'k-bubbles' as shown in Figure 15, which also have an inclination flip of type $\mathbf{C}_{\mathrm{in}}$. They account for the bifurcation curves that are missing. The complete bifurcation diagram is again an infinite puzzle of k-bubbles that are organized according to the order of bifurcations near the main codimension-two singularities $\mathbf{C}_{\mathrm{out}}$ and $\mathbf{C}_{\mathrm{in}}$, respectively. This order is the same as in the previous case and determined by the one-dimensional map as explained in Appendix A.

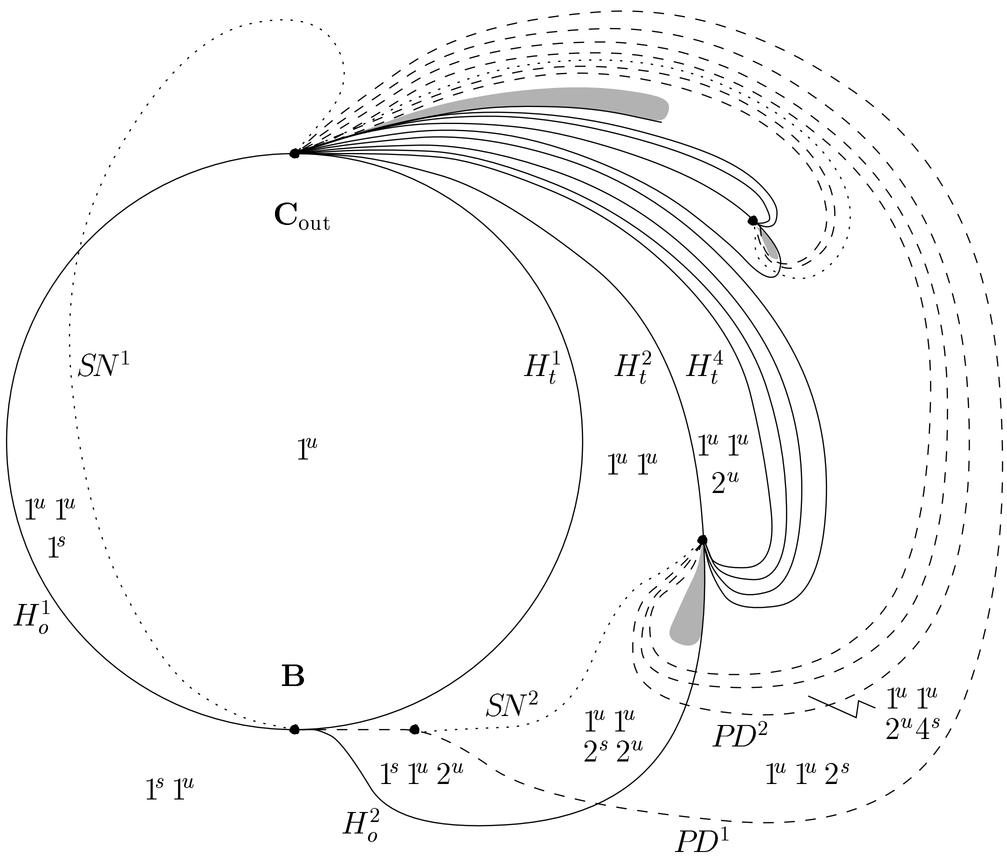

Figure 13: The transition from $\mathbf{B}$ to $\mathbf{C}_{\text{out}}$ via inclination flips of type $\mathbf{C}_{\text{in}}$.

4.4 From a homoclinic-doubling cascade to a point of type $\mathbf{C}_{\text{in}}$

It is of help to consider the transition of the spheres in Figures 10 and 11 to those in Figures 13 and 14 as β is changed through $1/2$, where the central singularity is an orbit flip. We picture this bifurcation as follows. Let $1/2 < \beta$ and consider decreasing β toward the bifurcation value $1/2$. Then the successive points in each homoclinic-doubling cascade move closer to each other. (Note that only one parameter should be necessary for this, because it is a reasonable conjecture that there is a scaling law just like in period-doubling.)

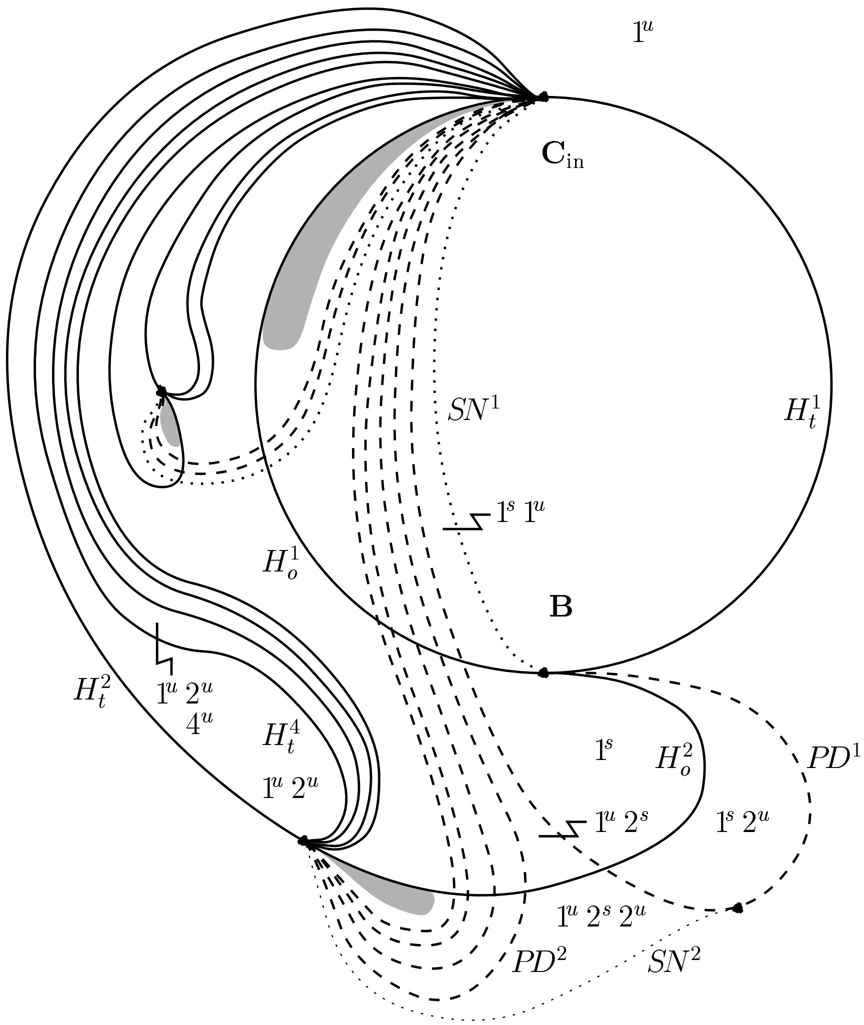

Figure 14: The transition from **B** to $\mathbf{C}_{\rm in}$ via inclination flips of type $\mathbf{C}_{\rm in}$.

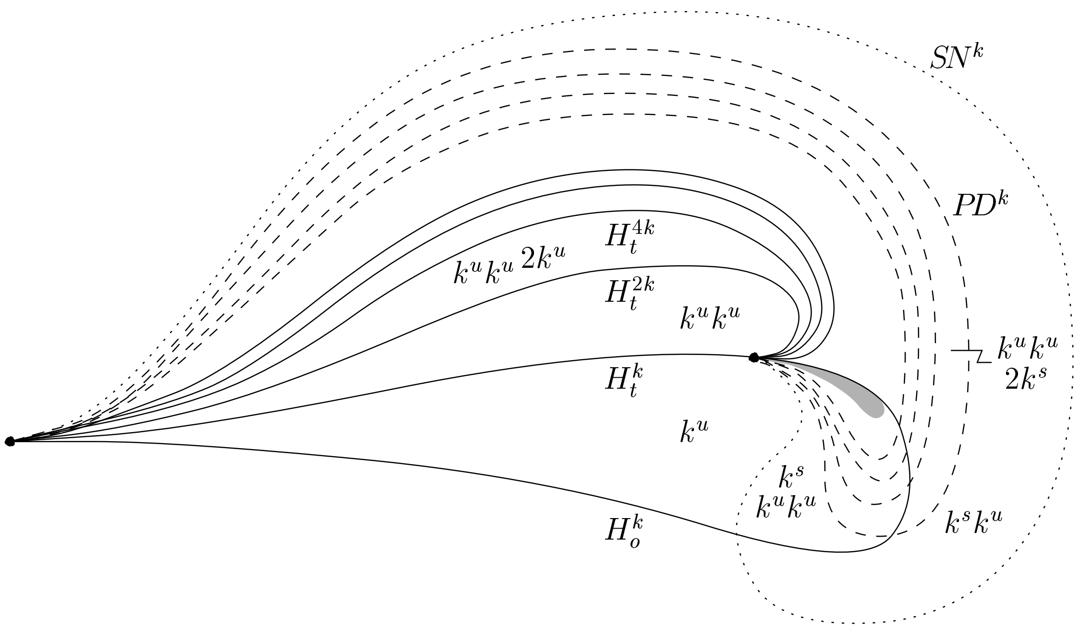

Figure 15: A k-bubble with an inclination flip of type $\mathbf{C}_{\text{in}}$.

When $\beta = 1/2$ each period doubling cascade has changed to a single point, which is an inclination flip of type $\mathbf{C}_{\text{in}}$. (An inclination flip of type $\mathbf{C}_{\text{out}}$ is not consistent with the number and stability of periodic orbits.) In order for this to happen, infinitely many cascades of the right combinatorics must all converge to the same point to form this inclination flip of type $\mathbf{C}_{\text{in}}$. We argue now that this ordering is already present 'in statu nascendi' for $1/2 < \beta$. Because the sphere is compact each homoclinic-doubling cascade has an accumulation point. (We conjecture that there is exactly one such point.) There are clearly infinitely many accumulation points of homoclinic-doubling cascades. We conjecture that the accumulation points of homoclinic-doubling cascades accumulate according to the requirement that they form inclination flips of type $\mathbf{C}_{\text{in}}$ as β crosses $1/2$. In fact, one could think of the accumulation points of accumulation points of homoclinic-doubling cascades as the seeds for $1/2 < \beta$ of the inclination flips of type $\mathbf{C}_{\text{in}}$ for $\beta < 1/2$. This creation of inclination flips of type $\mathbf{C}_{\text{in}}$ might be an explanation for certain computer generated pictures in [KKO95].

The infinite puzzle requires an infinite number of inclination flips for $\beta < 1/2$, which is in accordance with a result in [Nau96a]. Note that these inclination flips of type $\mathbf{C}_{\mathrm{in}}$ must also accumulate somewhere on the sphere, making the picture very intricate.

Acknowledgements

The authors thank H. Kokubu for fruitful discussions, and the Institute for Mathematics and its Applications, Minneapolis, for hospitality and support. B.K. acknowledges a travel grant from the Schwerpunktprogramm 'Ergodentheorie, Analysis und effiziente Simulation dynamischer Systeme' of the Deutsche Forschungsgemeinschaft.

References

[CDF90] Chow, S.-N., Deng, B., and Fiedler, B. (1990), Homoclinic bifurcation at resonant eigenvalues, *J. Dyn. Diff. Eq.* **2**, 177–244.

[Den89] Deng, B. (1989), The Shil'nikov problem, exponential expansion, strong λ-lemma, C^1-linearization, and homoclinic bifurcation, *Journ. Diff. Eq.* **79**, 189–231.

[Den89b] Deng, B. (1989), Exponential expansion with Šil'nikov's saddle-focus, *Journ. Diff. Eq.* **82**, 156–173.

[Den90] Deng B. (1993), Homoclinic twisting bifurcations and cusp horseshoe maps, *J. Dyn. Diff. Eq.* **5**, 417–467.

[DCFKSW97] Doedel, E.J., Champneys, A.R., Fairgrieve, T.F., Kuznetsov, Yu.A., Sandstede, B., and Wang, X. (1997), AUTO 97: Continuation and bifurcation sofware for ordinary diffential equations (with HomCont), `http://indy.cs.concordia.ca/auto/`

[DRS91] Dumortier, F., Roussarie, R., and Sotomayor, J. (1991), *Bifurcations of planar vector fields, nilpotent singularities and abelian integrals*, Lecture Notes in Mathematics **1480**, Springer Verlag.

[Hom96] Homburg, A.J. (1996), *Global aspects of homoclinic bifurcations of vector fields*, Memoirs of the A.M.S. **578**.

[HKK94] Homburg, A.J., Kokubu H., and Krupa, M. (1994), The cusp horseshoe and its bifurcations in the unfolding of an inclination flip homoclinic orbit, *Ergod. Th. & Dynam. Sys.* **14**, 667–693.

[HKN97] Homburg, A.J., Kokubu, H., and Naudot, V. (1997), Homoclinic-doubling cascades, preprint.

[KKO93a] Kisaka, M., Kokubu, H., and Oka, H. (1993), Bifurcations to N-homoclinic orbits and N-periodic orbits in vector fields, *J. Dyn. Diff. Eq.* **5**, 305–357.

[KKO93b] Kisaka, M., Kokubu, H., and Oka, H. (1993) Supplement to homclinic-doubling bifurcation in vector fields. In Bamon, R., Labarca, R., Lewowicz, J., and Palis, J. (eds.), *Dynamical Systems*, Longman, pp. 92–116.

[KKO95] Kokubu, H., Komuro, M., and Oka, H. (1995), Numerical study of a piecewise affine vector field, private communication.

[KKO96] Kokubu, H., Komuro, M., and Oka, H. (1996) Multiple homoclinic bifurcations from orbit flip. I. Successive homoclinic-doublings, *Int. J. Bif. Chaos* **6**, 833–850.

[KN97] Kokubu, H., and Naudot, V. (1997), Existence of infinitely many homoclinic-doubling bifurcations from some codimension-three homoclinic orbits, *J. Dyn. Diff. Eq.* **9**, 445–462.

[Ko95] Koper, M. (1995), Bifurcations of mixed-mode oscillations in a three-variable autonomous Van der Pol-Duffing model with a cross shaped phase diagram, Physica D **80**, 72–94.

[KR96] Krauskopf, B., and Rousseau, C. (1997), Codimension-three unfoldings of reflectionally symmetric vector fields, *Nonlinearity* **10**, 1115–1150.

[Mon96] Montealegre, M. (1996), *Bifurcações homoclínicas para selas em* $\mathbf{R}^3$ *com ressonância nas direções principais (Homoclinic bifurcations of saddles in* $\mathbf{R}^3$ *with resonance along principal directions)*, Ph.D.-thesis, Universidada de São Paulo; and personal communication with J. Sotmayor in 1998.

[Nii96] Nii, S. (1996), N-homoclinic bifurcations for homoclinic orbits changing their twisting, *J. Dyn. Diff. Eq.* **8**, 549–572.

[Nau96a] Naudot, V. (1996), *Bifurcations homoclines des champs de vecteurs en dimension trois*, Ph.D.-thesis, l'Université de Bourgogne, Dijon.

[Nau96b] Naudot, V. (1996), Strange attractor in the unfolding of an inclination flip homoclinic orbit, *Ergod. Th. & Dynam. Syst.* **16**, 1071–1086.

[Nau98] Naudot, V. (1998), A strange attractor in the unfolding of an orbit flip homoclinic orbit, preprint.

[OS87] Ovsyannikov, I.M., and Shil'nikov, L.P. (1987), On systems with saddle-focus homoclinic curve, *Math. USSR Sbornik*, **58**, 557–574.

[Rob89] Robinson, C. (1989), Homoclinic bifurcation to a transitive attractor of Lorenz type, *Nonlinearity* **2**, 495–518.

[Rob92] Robinson, C. (1992), Homoclinic bifurcation to a transitive attractor of Lorenz type. II, *SIAM J. Math. Anal.* **23**, 1255–1268.

[Rou93] Roussarie, R. (1993), Techniques in the theory of local bifurcations: cyclicity and desingularization, In Schlomiuk, D. (ed.), *Bifurcations and Periodic Orbits of Vector Fields*, NATO ASI Series C **408**, pp. 347–382.

[RR96] Roussarie, R., and Rousseau, C. (1996), Almost planar homoclinic loops in $\mathbf{R}^3$, *Journ. Diff. Eq.* **126**, 1–47.

[Ryc90] Rychlik, M.R. (1990), Lorenz attractors through Sil'nikov-type bifurcation. Part I, *Ergod. Th. & Dynam. Syst.* **10**, 793–821.

[San93] Sandstede, B. (1993) *Verzweigungstheorie homokliner Verdopplungen*, PhD-thesis, Free University of Berlin, Institut für Angewandte Analysis und Stochastic, Report No. 7, Berlin.

[San97] Sandstede, B. (1997), Constructing dynamical systems having homoclinic bifurcation points of codimension two, *J. Dyn. Diff. Eq.* **9**, 269–288.

[Shi65] Shil'nikov, L.P. (1965), A case of the existence of a countable number of periodic motions, *Soviet Math. Dokl.* **6**, 163–166.

[Shi67] Shil'nikov, L.P. (1967), On the Poincaré-Birkhoff problem, *Math. USSR Sbornik* **3**, 353–371.

[Sot98] Sotomayor, J. (1998), personal communication.

[Ste58] Sternberg, S. (1958), On the structure of local homeomorphisms of Euclidean n-space II, *Amer. Journ. Math.* **80**, 623–631.

[Yan87] Yanagida, E. (1987), Branching of double pulse solutions from single pulse solutions in nerve axon equations, *Journ. Diff. Eq.* **66**, 243–262.

[YA83] Yorke, J.A., and Alligood, K.T. (1983), Cascades of period doubling bifurcations: a prerequisite for horseshoes, *Bull. A.M.S.* **9**, 319–322.

[ZN98] Zimmerman, M.G., and Natiello, M.A. (1998), Global homoclinic and heteroclinic bifurcations close to a twisted heteroclinic cycle, *Int. J. Bif. Chaos* **8**(2), 359–376.

A Annihilation of horseshoes

In [HKK94] the destruction of horseshoes through sequences of homoclinic bifurcations in the unfolding of an inclination flip with the eigenvalue conditions $\alpha/\beta > 2$ and $\beta < 1/2$, was studied. This was done under a local linearizability assumption. In this appendix we wish to indicate, first, that the results in [HKK94] hold without the local linearizability assumption and, second, that similar bifurcation pictures exist both for the inclination flip with eigenvalue conditions $\alpha/\beta < 2$, $\alpha < 1$ and for the orbit flip with $\beta < \alpha < 1$. For the convenience of the reader we include a characterization of the order of the homoclinic bifurcations in which horseshoes are annihilated, where we follow [HKK94, Hom96].

A.1 Combinatorics of homoclinic orbits

Let us start with some considerations on the one-dimensional maps that appear as singular limits after a rescaling; see Section 2. The obtained interval maps, for the different flip homoclinic orbits, are all unimodal with a graph as depicted in Figure 8. Homoclinic bifurcations of X_μ correspond to periodic orbits of the interval map that contain 0. This follows from the fact that the local stable manifold of $\mathbf{0}$ becomes the point 0 in the reduction to the interval map. Note that an n-periodic orbit of the interval map that goes through 0 corresponds to an n-homoclinic orbit of X_μ. Kneading theory is the tool to obtain information on the set of periodic orbits, and hence, on the set of homoclinic bifurcations, when parameters are varied.

In order to explain this we consider a unimodal map f_μ with a minimum as in the left part of Figure 8. Similar considerations hold for unimodal maps with a maximum. As indicated in the figure, there is an interval $M = [0, m_\mu]$ that is mapped into itself by f_μ; the point m_μ is the rightmost fixed point of f_μ. Denote by c_μ the critical point of f_μ. For each point x, an itinerary $\mathcal{I}(x)$ is defined as a finite or infinite sequence $\mathcal{I}_j(x)$, $j \geq 0$, of symbols L and R, according to the following rule.

$$\mathcal{I}_j(x) = \begin{cases} L, & \text{if } f_\mu^j(x) < c_\mu, \\ R, & \text{if } f_\mu^j(x) > c_\mu. \end{cases}$$

If $f_\mu^j(x)$ is outside of M, i.e. if $f_\mu^j(x) < 0$ or if $f_\mu^j(x) > m_\mu$, then $\mathcal{I}_k(x)$ is not defined for $k \geq j + 1$.

One defines an ordering on itineraries as follows. Let $\mathcal{I}$, $\mathcal{J}$ be two itineraries. Then $\mathcal{I} < \mathcal{J}$ if for the first integer j with $\mathcal{I}_j \neq \mathcal{J}_j$, the following holds: either $\mathcal{I}_j = L$ and $\mathcal{J}_j = R$ and the number of L's in $\mathcal{I}_i$, $0 \leq i < j$ is odd, or $\mathcal{I}_j = R$ and $\mathcal{J}_j = L$ and the number of L's in $\mathcal{I}_i$, $0 \leq i < j$ is even.

Note that $f_\mu^j(x)$ is decreasing at x (and thus changes the order of points close to x), precisely if the number of L's in $\mathcal{I}_i(x)$, $0 \leq i \leq j$ is odd. From this one deduces that $\mathcal{I}(x) < \mathcal{I}(y)$ implies $x < y$, so that itineraries of points reflect the position on the interval. This observation immediately gives a result on the order of homoclinic bifurcations. First note that if for μ_1 a fixed small number, one lets μ_2 increase, a horseshoe is created. Indeed, for $\mu_2 = 0$ we have $f_\mu(0) = 0$ and therefore the invariant set of f_μ consists of a fixed point in 0 (corresponding to a homoclinic orbit for X_μ) and a fixed point in m_μ (a periodic orbit for X_μ), whereas for some positive value of μ_2 one has $f_\mu(0) = m_\mu$ and so f_μ possesses a horseshoe. From the above considerations one concludes that for each $\mathcal{I} < \mathcal{J}$, there are parameter values $\mu_2^1 < \mu_2^2$ (recall that μ_1 is small and fixed), so that 0 is a periodic point both for $f_{(\mu_1,\mu_2^1)}$ and for $f_{(\mu_1,\mu_2^2)}$, and such that $\mathcal{I}(0) = \mathcal{I}$ for $\mu = (\mu_1, \mu_2^1)$ and $\mathcal{I}(0) = \mathcal{J}$ for $\mu = (\mu_1, \mu_2^2)$. If one further has a monotonicity property of the homoclinic bifurcations, saying that the value of μ_2 (for fixed μ_1) for which 0 is periodic with some prescribed itinerary, is unique, then this fully describes the order of homoclinic bifurcations.

We now show that f_μ has such a monotonicity property; see also [HKK94]. By the chain rule,

$$\frac{\partial}{\partial \mu_2} f_\mu^n \big|_x \quad = \quad \sum_{j=0}^{n-1} \frac{d}{dx} f_\mu^j \Big|_{f_\mu^{n-j}(x)} \frac{\partial}{\partial \mu_2} f_\mu \Big|_{f_\mu^{n-j-1}(x)} .$$

Since for μ small, $|\frac{d}{dx} f_\mu|_x|$ is large, the above expression is nonzero and its sign equals the sign of the dominant term $\frac{d}{dx} f_\mu^{n-1}\Big|_{f_\mu(x)} \frac{\partial}{\partial \mu_2} f_\mu|_x$. Applying this to $x = 0$ at a homoclinic bifurcation value, shows the required monotonicity.

Following [Hom96], one sees that the first homoclinic bifurcations are of periodic points with itineraries

$$(L)^\infty, \; (LR)^\infty, \; (LRLL)^\infty, \; (LRLLLRLR)^\infty,$$

in this order. For each itinerary, the following itinerary is obtained by taking the block of symbols which is periodically repeated, putting two of these blocks behind eachother, changing the last symbol of the new obtained block and then repeat this block periodically. There are various of such sequences of homoclinic bifurcations. Indeed, if U is a block of symbols containing an even number of L's, then there is a sequence of subsequent homoclinic bifurcations with the following itineraries:

$$(UR)^\infty,\ \ (UL)^\infty,\ \ (ULUR)^\infty,\ \ (ULURULUL)^\infty,$$

and so on using the same rule as above. A similar sequence of subsequent homoclinic bifurcations exists for blocks of symbols U containing an odd number of L's. Here the order is

$$(UL)^\infty,\ \ (UR)^\infty,\ \ (URUL)^\infty,\ \ (URULURUR)^\infty,$$

and so on.

A.2 Strong stable foliations

Recall that f_μ is the singular limit of a rescaled return map $\bar{\Phi}$ as $\mu_1 \to 0$. The above results on the one-dimensional map can be extended to $\bar{\Phi}$, by constructing a strong stable foliation. Identifying points on the same leaf of such a foliation, results in a one-dimensional map, close to f_μ for μ small. To extend the combinatorial part of the above description to $\bar{\Phi}$, it suffices to construct a continuous strong stable foliation: kneading theory applies to continuous unimodal maps. To extend statements on monotonicity and genericity of the unfolding of the bifurcations, a continuously differentiable strong stable foliation is required.

We now prove for the case of the orbit flip that a continuously differentiable strong stable foliation for $\bar{\Phi}$ does exist. Similar proofs can be given for the two types of inclination flips. Recall from Section 2 that, for μ_1 small, the rescaled return map $(\bar{x}_s, \bar{x}_u) \mapsto \bar{\Phi}(\bar{x}_s, \bar{x}_u)$ is a singular perturbation from the one-dimensional map

$$\bar{x}_u \ \ \mapsto \ \ \begin{pmatrix} A\bar{x}_u^\alpha + B\bar{x}_u^\beta \\ |\mu_1|^{\frac{\alpha-1}{\alpha-\beta}} g(\bar{x}_u) \end{pmatrix},$$

where $g(\bar{x}_u) = s + C\bar{x}_u^\alpha + D\mathrm{sign}(\mu_1)\bar{x}_u^\beta$.

In order to state the result we consider $(\bar{x}_s, \bar{x}_u)$ on a bounded region $[-l, l] \times (0, k]$, for some k, l large enough. Related or comparable results can be found in [Rob89, Rob92, Ryc90, HKK94, Hom96].

Proposition A.1 *For some $\lambda > 0$, and $D\mu_1$ of the opposite sign as C, let W be the set of parameter values so that $\left| g'|_I \right| \geq \lambda$, where $I = \{\bar{x}_u \in (0,k]; \quad |\mu_1|^{\frac{\alpha-1}{\alpha-\beta}} g(\bar{x}_u) \in (0,k]\}$. For $(\mu_1,\mu_2) \in W$, $\bar{\Phi}$ possesses a C^1 strong stable foliation on $[-l,l] \times [0,k]$. This foliation depends C^1-smoothly on μ_2 and continuously on μ_1.*

Proof. Instead of studying the Poincaré return map Φ on $D_{\mu_1} \subset \Sigma^{in}$ (where D_{μ_1} is the box that rescales to $[-l,l] \times (0,k]$), we consider the Poincaré return map Ψ on the parameter dependent cross section

$$S^{in} = \{x_s = \mu_1, |x_{ss}|, |x_u| \leq 1\}.$$

This makes the construction similar to corresponding constructions near inclination flip homoclinic orbits. Note that for $\mu_2 = 0$ the homoclinic orbit intersects S^{in} in $(1, \mu_1, 0)$. For definiteness we assume that C and D are such that μ_1 is positive. Let

$$E_{\mu_1} = \{0 < x_u \leq k\mu_1^{\sigma}, |x_{ss} - 1| \leq l\mu_1^{\nu}\},$$

$\sigma = 1/(\alpha - \beta)$, $\nu = \alpha/(\alpha - \beta)$, be a small box in S^{in}. The existence of a strong stable foliation for Φ on D_{μ_1} follows from the existence of a strong stable foliation for Ψ on E_{μ_1}.

A strong stable foliation is obtained by integrating a line field that is invariant under $D\Psi$ and has the property that $D\Psi$ strongly contracts vectors in the direction of the line field. Such a line field is constructed using an appropriate graph transform. We first prove the proposition for fixed parameter values, and after that indicate how parameter dependence is treated. Take rescaled coordinates $(\bar{x}_{ss}, \bar{x}_u) \in [-l,l] \times (0,k]$ on E_{μ_1} given by

$$\begin{aligned} x_{ss} - 1 &= \mu_1^{\nu} \bar{x}_{ss}, \\ x_u &= \mu_1^{\sigma} \bar{x}_u, \end{aligned}$$

and let $\bar{\Psi}$ denote the Poincaré return map in these rescaled coordinates. Write $T([-l,l] \times (0,k]) = [-l,l] \times (0,k] \times E^{ss} \times E^u$. Let $\bar{\boldsymbol{\Psi}}^{-1}$ be the map induced by $\bar{\Psi}^{-1}$ on $[-l,l] \times (0,k] \times \mathcal{L}(E^{ss}, E^u)$;

$$\bar{\boldsymbol{\Psi}}^{-1}(\bar{x}_{ss}, \bar{x}_u, \bar{v}) = (\bar{\Psi}^{-1}(\bar{x}_{ss}, \bar{x}_u), \bar{w}),$$

with

$$\text{graph } \bar{w} = D\bar{\Psi}^{-1}(\bar{x}_{ss}, \bar{x}_u) \text{graph } \bar{v}.$$

Let Γ be the corresponding graph transform on $C^0([-l,l]\times(0,k],\mathcal{L}(E^{ss},E^u))$, that is, Γ is defined by

$$(\bar{x}_{ss},\bar{x}_u,\Gamma(\bar{v})(\bar{x}_{ss},\bar{x}_u)) \quad = \quad \bar{\mathbf{\Psi}}^{-1}(\bar{\Psi}(\bar{x}_{ss},\bar{x}_u),\bar{v}\circ\bar{\Psi}(\bar{x}_{ss},\bar{x}_u))$$

for $(\bar{x}_{ss},\bar{x}_u)$ such that $\bar{\Psi}(\bar{x}_{ss},\bar{x}_u)\in[-l,l]\times(0,k]$. For other $(\bar{x}_{ss},\bar{x}_u)$ we let $\Gamma(\bar{v})(\bar{x}_{ss},\bar{x}_u)=\bar{v}_0(\bar{x}_{ss},\bar{x}_u)$ for a fixed section $\bar{v}_0$; see [HKK94, Hom96] for details.

We claim the existence of a positive function δ on $[-l,l]\times[0,k]$ with $\delta(\bar{x}_{ss},0)=0$, so that

- Γ maps $\mathrm{Lip}_\delta([-l,l]\times(0,k],\mathcal{L}(E^{ss},E^u))$ into itself.
- Γ is a contraction on $\mathrm{Lip}_\delta([-l,l]\times(0,k],\mathcal{L}(E^{ss},E^u))$ in the supnorm.

Here Lip_δ stands for Lipschitz continuous sections with Lipschitz constant $\delta(x)$ at the point x. Because $\bar{\Psi}$ is only defined for $\bar{x}_u>0$ (and at $\bar{x}_u=0$ by continuous extension), we consider Lipschitz functions with a Lipschitz constant that depends on the point and is small for small $\bar{x}_u$. The fact that Γ is a contraction on $\mathrm{Lip}_\delta([-l,l]\times(0,k],\mathcal{L}(E^{ss},E^u))$, with the properties of δ, implies the existence of a continuous strong stable foliation.

Moreover, we claim that for some positive constants $\epsilon<1$ and M that

- Γ maps $\mathrm{Lip}_\delta([-l,l]\times(0,k],\mathcal{L}(E^{ss},E^u))\cap C^{1+\epsilon}_M([-l,l]\times(0,k],\mathcal{L}(E^{ss},E^u))$ into itself.

Here $C^{1+\epsilon}_M$ stands for continuously differentiable sections whose derivatives are ϵ-Hölder with Hölder constant M. Since the intersection of this space of $C^{1+\epsilon}_M$ sections with that of Lip_δ sections is a closed subspace of $C^0([-l,l]\times(0,k],\mathcal{L}(E^{ss},E^u))$ in the supnorm (see for example [Hom96]) the existence of a $C^{1+\epsilon}$ strong stable foliation follows from the claims.

In the remainder, we prove the claims. From Proposition B.5 in Appendix B (or from very similar reasonings), one has

$$\bar{\Psi}(\bar{x}_{ss},\bar{x}_u)= \begin{pmatrix} A(\bar{x}_{ss})\bar{x}_u^\alpha+B(\bar{x}_{ss})\mu_1\bar{x}_u^\beta+\mathcal{O}(|\mu_1|^\omega\bar{x}_u^{\beta+\omega}) \\ |\mu_1|^{\frac{\alpha-1}{\alpha-\beta}}\left(C(\bar{x}_{ss})\bar{x}_u^\alpha+D(\bar{x}_{ss})\mu_1\bar{x}_u^\beta+\mathcal{O}(|\mu_1|^\omega\bar{x}_u^{\beta+\omega})\right)\end{pmatrix} \tag{9}$$

for some $\omega>0$. The higher order terms can be differentiated, as stated in Proposition B.5. The function A is of the form $\tilde{A}(1+|\mu_1|^\nu\bar{x}_{ss})$ for a smooth function $\tilde{A}$. Similarly for B,C,D.

Consider the action of the map $\bar{\mathbf{\Psi}}^{-1} : \bar{\Psi}([-l,l]\times(0,k))\times\mathcal{L}(E^{ss},E^u) \to [-l,l]\times(0,k]\times\mathcal{L}(E^{ss},E^u)$, induced by $\bar{\Psi}^{-1}$. Write

$$D\bar{\Psi}(\bar{x}_{ss},\bar{x}_u) = \begin{pmatrix} a(\bar{x}_{ss},\bar{x}_u) & b(\bar{x}_{ss},\bar{x}_u) \\ c(\bar{x}_{ss},\bar{x}_u) & d(\bar{x}_{ss},\bar{x}_u) \end{pmatrix}.$$

Observe that $\bar{\mathbf{\Psi}}^{-1}(\bar{\Psi}(\bar{x}_{ss},\bar{x}_u),w) = (\bar{x}_{ss},\bar{x}_u,v)$, where w and v are related by

$$\begin{pmatrix} a(\bar{x}_{ss},\bar{x}_u) & b(\bar{x}_{ss},\bar{x}_u) \\ c(\bar{x}_{ss},\bar{x}_u) & d(\bar{x}_{ss},\bar{x}_u) \end{pmatrix}\begin{pmatrix} 1 \\ v \end{pmatrix} = k\begin{pmatrix} 1 \\ w \end{pmatrix}$$

for some $k \in \mathbf{R}$. This shows that v and w are related by

$$v = \frac{-c(\bar{x}_{ss},\bar{x}_u) + a(\bar{x}_{ss},\bar{x}_u)w}{d(\bar{x}_{ss},\bar{x}_u) - b(\bar{x}_{ss},\bar{x}_u)w}.$$

So, if $\bar{v} \in C^0(\bar{\Psi}([-l,l]\times(0,k]),\mathcal{L}(E^{ss},E^u))$ then

$$\Gamma(\bar{v}) = \frac{-c + a\bar{v}\circ\bar{\Psi}}{d - b\bar{v}\circ\bar{\Psi}}.$$

Write $\mathcal{O} = \mathcal{O}(|\mu_1|^\omega \bar{x}_u^{\beta+\omega})$, $\mathcal{O}_1 = \mathcal{O}(|\mu_1|^\omega \bar{x}_u^{\beta+\omega-1})$, $\mathcal{O}_2 = \mathcal{O}(|\mu_1|^\omega \bar{x}_u^{1+\omega})$ and $\mathcal{O}_3 = \mathcal{O}(|\mu_1|^\omega \bar{x}_u^{\omega})$. Using (9) one computes

$$\Gamma(\bar{v})(\bar{x}_{ss},\bar{x}_u) =$$

$$\frac{-|\mu_1|^{\frac{\alpha-1}{\alpha-\beta}}\left[C'\bar{x}_u^\alpha + \operatorname{sign}(\mu_1)D'\bar{x}_u^\beta + \mathcal{O}\right] + \left(A'\bar{x}_u^\alpha + B'\bar{x}_u^\beta + \mathcal{O}\right)\bar{v}\circ\bar{\Psi}}{-|\mu_1|^{\frac{\alpha-1}{\alpha-\beta}}\left[C\alpha\bar{x}_u^\alpha + \operatorname{sign}(\mu_1)D\beta\bar{x}_u^\beta + \mathcal{O}_1\right] + \left(A\alpha\bar{x}_u^\alpha + B\beta\bar{x}_u^\beta + \mathcal{O}_1\right)\bar{v}\circ\bar{\Psi}}$$

$$\frac{-C'\bar{x}_u^{1+\alpha-\beta} - \operatorname{sign}(\mu_1)D'\bar{x}_u + \mathcal{O}_2 + |\mu_1|^{\frac{1-\alpha}{\alpha-\beta}}\left(A'\bar{x}_u^{1+\alpha-\beta} + B'\bar{x}_u + \mathcal{O}_2\right)\bar{v}\circ\bar{\Psi}}{-C\alpha\bar{x}_u^{\alpha-\beta} - \operatorname{sign}(\mu_1)D\beta + \mathcal{O}_3 - |\mu_1|^{\frac{1-\alpha}{\alpha-\beta}}\left(A\alpha\bar{x}_u^{\alpha-\beta} + B\beta + \mathcal{O}_3\right)\bar{v}\circ\bar{\Psi}}$$

Here A, B, C, D and their derivatives are computed in $\bar{x}_{ss}$ and $\bar{v}\circ\bar{\Psi}$ is computed in $(\bar{x}_{ss},\bar{x}_u)$.

By assumption, $-\bar{x}_u^{1-\beta}g'(\bar{x}_u) \sim -C\alpha\bar{x}_u^{\alpha-\beta} - \operatorname{sign}(\mu_1)D\beta$ (the term appearing in the denominator of the above expression) is bounded away from zero. Note further that $\Gamma(\bar{v})(\bar{x}_{ss},0) = 0$. From these facts one derives the existence of a positive function δ with $\delta(\bar{x}_{ss},0) = 0$, so that Γ maps Lip_δ sections to Lip_δ sections. It is also clear that Γ is a contraction on Lip_δ for μ_1 small. By differentiating the above expression one can show that Γ moreover maps $C_M^{1+\epsilon}$ sections to $C_M^{1+\epsilon}$ sections for suitable ϵ, M, compare [HKK94].

Regularity with respect to the parameters follows from similar reasonings by considering the map $(\bar{x}_{ss},\bar{x}_u,\mu_1,\mu_2) \mapsto (\bar{\Psi}(\bar{x}_{ss},\bar{x}_u),\mu_1,\mu_2)$, see [HKK94].

□

B Exponential expansions

In this appendix we provide exponential expansions for the local transition maps for the vector field X_μ encountered in Section 2. It is well known that under the assumption of nonresonance conditions on the eigenvalues of $DX_\mu(\mathbf{0})$, there exist smooth coordinates near $\mathbf{0}$ in which X_μ is linear [Ste58]. For a locally linear vector field, an explicit expression for the local transition map can be given. Since we consider resonant flip bifurcations, and thus have rationally dependent eigenvalues, we can not assume the existence of smooth locally linearizing coordinates. We circumvent this difficulty by computing asymptotic expansions for the local transition maps. This provides a way to study homoclinic bifurcations without having to rely on the simplifying assumption of smooth local linearizability. We start with a normal form theorem.

Let X_μ be given by a set of ordinary differential equations

$$\begin{aligned} \dot{x_{ss}} &= -\alpha x_{ss} + F_{ss}(x_{ss}, x_s, x_u), \\ \dot{x_s} &= -\beta x_s + F_s(x_{ss}, x_s, x_u), \\ \dot{x_u} &= x_u + F_u(x_{ss}, x_s, x_u), \end{aligned} \tag{10}$$

where F^{ss}, F^s, F^u are quadratic and higher order terms.

Lemma B.1 *The vector field X_μ is smoothly equivalent to a vector field of the same form with*

$$\begin{aligned} F_{ss}(x_{ss}, x_s, x_u) &= \mathcal{O}(\|(x_{ss}, x_s)\|^2), \\ F_s(x_{ss}, x_s, x_u) &= x_u\mathcal{O}(|x_{ss}| + \|(x_{ss}, x_s)\|^2), \\ F_u(x_{ss}, x_s, x_u) &= 0. \end{aligned}$$

Moreover, if $\alpha > 2\beta$, the same is true with

$$F_{ss}(x_{ss}, x_s, x_u) = \mathcal{O}(x_{ss}^2 + |x_{ss}x_s| + x_s^3).$$

If $\alpha - \beta < 1$, we can take

$$F_s(x_{ss}, x_s, x_u) = \mathcal{O}(\|(x_{ss}, x_s)\|^2).$$

Proof. By a smooth coordinate change, the local stable and unstable manifolds are linear. Then F_{ss} and F_s are of order $\mathcal{O}(\|x_{ss}, x_s\|)$ and F_u is of order $\mathcal{O}(|x_u|)$. Multiplying the vector field with the smooth function $x_u/(x_u+F_u(x_{ss}, x_s, x_u))$, we obtain that X_μ is smoothly equivalent to a vector field for which $F_u = 0$.

First, by some smooth cordinate transformation, we remove terms $x_{ss}x_u$ from the differential equation for x_{ss} and terms $x_s x_u$ from the differential equation for x_s. For this, consider a coordinate change $(x_{ss}, x_s, x_u) \mapsto (y_{ss}, y_s, y_u)$ of the form

$$\begin{aligned} y_{ss} &= x_{ss} + p^{ss}(x_u)x_{ss}, \\ y_s &= x_s + q^s(x_u)x_s, \\ y_u &= x_u, \end{aligned}$$

for functions p^{ss}, p^s which vanish at $x_u = 0$. Write the differential equations in the new coordinates (y_{ss}, y_s, y_u) as

$$\begin{aligned} \dot{y_{ss}} &= -\alpha y_{ss} + G^{ss}(y_{ss}, y_s, y_u)y_{ss} + G^s(y_{ss}, y_s, y_u)y_s, \\ \dot{y_s} &= -\beta y_s + H^{ss}(y_{ss}, y_s, y_u)y_{ss} + H^s(y_{ss}, y_s, y_u)y_s, \\ \dot{y_u} &= y_u. \end{aligned}$$

At $y_{ss}, y_s = 0$, we have

$$\begin{aligned} G^{ss}(0,0,y_u) &= \dot{p^{ss}} + h.o.t., \\ H^s(0,0,y_u) &= \dot{q^s} + h.o.t., \end{aligned}$$

where $h.o.t.$ stands for higher order terms in (p^{ss}, q^s, y_u), compare [OS87, Den89b]. We seek functions p^{ss}, q^s of $y_u = x_u$ so that G^{ss} and H^s vanish at $y_{ss}, y_s = 0$. Considering p^{ss} and q^s as variables, this yields differential equations for (p^{ss}, q^s, y_u):

$$\begin{aligned} \dot{p}^{ss} &= h.o.t., \\ \dot{q}^s &= h.o.t., \\ \dot{y}_u &= y_u. \end{aligned}$$

The eigenvalues of the linearized differential equations, at $p^{ss}, q^s, y_u = 0$, are $0, 0, 1$. Hence we obtain the desired functions p^{ss}, q^s by constructing the one-dimensional strong unstable manifold for the above system of differential equations.

On the stable manifold, there exists a strong stable foliation with one dimensional leaves, extending the strong stable manifold. A smooth coordinate change brings this foliation into an affine foliation. The differential equation for x_s restricted to the stable manifold $\{x_u = 0\}$ depends only on x_s. Since one-dimensional vector fields can always be smoothly linearized near a sink, after a smooth coordinate change we get $F_s(x_{ss}, x_s, x_u) = \mathcal{O}(|x_u|\|(x_{ss}, x_s)\|)$. Any center unstable manifold $W^{s,u}(\mathbf{0})$ has the same tangent bundle along $W^u(\mathbf{0})$, see for example [Hom96]. By a smooth coordinate change $TW^{s,u}(\mathbf{0})\Big|_{W^u(\mathbf{0})} = T\{x_{ss} = 0\}$. This removes terms $x_s x_u$ from the differential equation for x_{ss}. If $\alpha > 2\beta$ then any $W^{s,u}(\mathbf{0})$ is a C^2 manifold and has a unique bundle of 2-jets along $W^u(\mathbf{0})$. A smooth coordinate change makes any $W^{s,u}(\mathbf{0})$ second-order tangent to $\{x_{ss} = 0\}$ along $W^u(\mathbf{0})$. Then also terms x_s^2 and $x_s^2 x_u$ from the differential equation for x_{ss} are removed. Also, if $\alpha - \beta < 1$ then there is a smooth plane bundle along $W^u(\mathbf{0})$, extending $T_{\mathbf{0}}W^{ss}(\mathbf{0}) \oplus T_{\mathbf{0}}W^u(\mathbf{0}) = \{x_s = 0\}$ over the origin; compare for example [HKN97]. A smooth coordinate change makes this plane bundle constant. Terms $x_{ss}x_u$ are absent from the differential equation for x_s after such a coordinate change. None of the coordinate changes destroys the results of the earlier coordinate changes, so that the lemma is proved. □

B.1 Exponential expansions for the inclination-flip

Recall that $\Sigma^{in} = \{x_s = 1\}$ and $\Sigma^{out} = \{x_u = 1\}$. The following proposition provides asymptotic expansions of the local transition map $\Phi_{loc} : \Sigma^{in} \to \Sigma^{out}$. Its proof relies on an improvement of estimates derived in [OS87, Den89, Den89b].

Proposition B.2 *Suppose $2\beta \neq \alpha$. Then, after a smooth local coordinate change, $\Phi_{loc} : \Sigma^{in} \to \Sigma^{out}$ has the following expression for its components $\Phi_{loc} = (\Phi_{loc}^{ss}, \Phi_{loc}^{s})$:*

$$\begin{aligned}
\Phi_{loc}^{ss}(x_{ss}, x_u) &= x_u^{\min\{\alpha, 2\beta\}}\left(\psi^{ss}(x_{ss}) + R^{ss}(x_{ss}, x_u)\right), \\
\Phi_{loc}^{s}(x_{ss}, x_u) &= x_u^{\beta}\left(\psi^{s}(x_{ss}) + R^{s}(x_{ss}, x_u)\right).
\end{aligned}$$

The functions ψ^{ss}, ψ^s are smooth, $\psi^s \neq 0$ and $\psi^{ss}(0) = 0$ if $\alpha < 2\beta$.

Furthermore, R^{ss} and R^s are smooth for $x_u > 0$; for some $\sigma > 0$, there exist constants $C_{k+l} > 0$ so that with $i = ss, s$

$$\left| \frac{\partial^{k+l}}{\partial x_u^k \partial (x_{ss}, \mu)^l} R^i(x_{ss}, x_u) \right| \leq C_{k+l} x_u^{\sigma - k} .$$

Proof. We give the proof under the assumption that $\alpha > 2\beta$. The proof for case $\alpha < 2\beta$ is similar; compare [HKN97].

For $\tau > 0$ and ξ_s with $|\xi_{ss}| < 1$, let

$$x(t, \tau, \xi_{ss}) = (x_{ss}, x_s, x_u)(t, \tau, \xi_{ss})$$

be an orbit of X_μ with

$$\begin{aligned} x_{ss}(0, \tau, \xi_{ss}) &= \xi_{ss}, \\ x_s(0, \tau, \xi_{ss}) &= 1, \\ x_u(\tau, \tau, \xi_s) &= 1. \end{aligned}$$

These conditions uniquely define the orbit $x(t, \tau, \xi_{ss})$; see [Shi67, Den89]. We will first show the following lemma, providing estimates on $x_{ss}(t, \tau, \xi_{ss})$ and $x_s(t, \tau, \xi_{ss})$.

Lemma B.3 *For $k \geq 0$, there are positive constants C_k so that, for $0 \leq t \leq \tau$ and μ near 0,*

$$\begin{aligned} \left| \frac{\partial^k}{\partial (t, \xi_{ss}, \mu)^k} x_{ss}(t, \tau, \xi_{ss}) \right| &\leq C_k e^{-2\beta t}, \\ \left| \frac{\partial^k}{\partial (t, \xi_{ss}, \mu)^k} x_s(t, \tau, \xi_{ss}) \right| &\leq C_k e^{-\beta t}. \end{aligned}$$

Furthermore, for the derivatives with respect to τ,

$$\begin{aligned} \left| \frac{\partial^k}{\partial (t, \tau, \xi_{ss}, \mu)^k} \frac{\partial}{\partial \tau} x_{ss}(t, \tau, \xi_{ss}) \right| &\leq C_k e^{-2\beta t + (t-\tau)}, \\ \left| \frac{\partial^k}{\partial (t, \tau, \xi_{ss}, \mu)^k} \frac{\partial}{\partial \tau} x_s(t, \tau, \xi_{ss}) \right| &\leq C_k e^{-\beta t + (t-\tau)}. \end{aligned}$$

Proof of Lemma B.3. To simplify the notation we write for example $x(t)$ for $x(t,\tau,\xi_{ss})$. Let δ be the distance of the sections Σ^{in} and Σ^{out} to the origin, before rescaling. Because of the applied rescaling $(x_{ss},x_s,x_u) \mapsto (x_{ss},x_s,x_u)/\delta$, we have

$$|F^{ss}(x_{ss},x_s,x_u)|\,,|F^{s}(x_{ss},x_s,x_u)| \;\leq\; C\delta, \tag{11}$$

for some $C > 0$ uniformly in (x_{ss},x_s,x_u,μ). By the variation of constants formula

$$x_{ss}(t) \;=\; e^{-\alpha t}\xi_{ss} + \int_0^t e^{-\alpha(t-s)}F^{ss}(x(s))ds, \tag{12}$$

$$x_s(t) \;=\; e^{-\beta t} + \int_0^t e^{-\beta(t-s)}F^{s}(x(s))ds. \tag{13}$$

For $\kappa,\lambda > 0$ and a finite dimensional vector space E with norm $\|\cdot\|$, let

$$\Sigma_{\kappa,\lambda}([0,\tau],E) \;=\; \{y \in C^0([0,\tau],E);\quad \sup_{0\leq t\leq \tau}\|y(t)\|e^{\kappa t+\lambda(\tau-t)} < \infty\}.$$

Equipped with the norm

$$\|y\|_{\kappa,\lambda} \;=\; \sup_{0\leq t\leq\tau}\|y(t)\|e^{\kappa t+\lambda(\tau-t)}$$

$\Sigma_{\kappa,\lambda}([0,\tau],E)$ is a Banach space.

Let $\mathcal{Y} = (\mathcal{Y}^{ss},\mathcal{Y}^{s})$ be the map on $C^0([0,\tau],\mathbf{R}^2)$ that maps (x_{ss},x_s) to the right hand side of (12), (13). Let $\mathbf{B}_R$ denote the ball of radius R in $\Sigma_{\alpha,0}([0,\tau],\mathbf{R})\times\Sigma_{\beta,0}([0,\tau],\mathbf{R})$. We claim that for $\|\xi_s\| \leq 1$ there exists $R > 0$ so that

- $\mathcal{Y}$ maps $\mathbf{B}_R$ inside itself,
- $\mathcal{Y}$ is a contraction on $\mathbf{B}_R$.

The fixed point of $\mathcal{Y}$, providing the orbit x, therefore satisfies the estimates in the statement of the lemma.

The claim is obtained using (11) and lemma B.1. Since the arguments closely follow those in [Den89], we leave performing these estimates to the reader. One treats (higher order) derivatives by differentiating (12), (13) and using the obtained identities to define a map on an appropriate weighted Banach space. Performing estimates as above one shows that this map is a contraction on some ball in the weighted Banach space. For details we refer to [Den89]. □

To obtain more precise asymptotics, we study the functions

$$\begin{aligned} z_{ss}(u,\tau,\xi_{ss}) &= e^{2\beta(\tau-u)}x_{ss}(\tau-u,\tau,\xi_{ss}), \\ z_s(u,\tau,\xi_{ss}) &= e^{\beta(\tau-u)}x_s(\tau-u,\tau,\xi_{ss}), \end{aligned}$$

for which we have the following.

Lemma B.4 *The limit functions*

$$\begin{aligned} z_{ss}^{\infty}(u,\xi_{ss}) &= \lim_{\tau\to\infty} z_{ss}(u,\tau,\xi_{ss}), \\ z_s^{\infty}(u,\xi_{ss}) &= \lim_{\tau\to\infty} z_s(u,\tau,\xi_{ss}) \end{aligned}$$

exist as smooth functions of (u,ξ_{ss}). *For any* $0<\sigma^{ss}<\alpha(0)-2\beta(0)$ *and* $0<\sigma^s<\min\{\alpha(0)-\beta(0),\beta(0)\}$, *there are* C_k *so that for* $0\le u\le\tau$ *and* μ *small*

$$\begin{aligned} \left|\frac{\partial^k}{\partial(u,\tau,\xi_{ss},\mu)^k}\left(z_{ss}(u,\tau,\xi_{ss})-z_{ss}^{\infty}(u,\xi_{ss})\right)\right| &\le C_k e^{\sigma^{ss}(u-\tau)}, \\ \left|\frac{\partial^k}{\partial(u,\tau,\xi_{ss},\mu)^k}\left(z_s(u,\tau,\xi_{ss})-z_s^{\infty}(u,\xi_{ss})\right)\right| &\le C_k e^{\sigma^{s}(u-\tau)}. \end{aligned}$$

Proof of Lemma B.4. We first show that

$$\left|\frac{\partial}{\partial\tau}z_{ss}(u,\tau,\xi_{ss})\right| \le Ce^{\sigma^{ss}(u-\tau)}, \tag{14}$$

$$\left|\frac{\partial}{\partial\tau}z_{s}(u,\tau,\xi_{ss})\right| \le Ce^{\sigma^{s}(u-\tau)}, \tag{15}$$

for some C. From this it follows that $z_{ss}^{\infty}(u,\xi_{ss})=\lim_{\tau\to\infty}z_{ss}(u,\tau,\xi_{ss})$ and $z_s^{\infty}(u,\xi_{ss})=\lim_{\tau\to\infty}z_s(u,\tau,\xi_{ss})$ exist, and that

$$\begin{aligned} |z_{ss}(u,\tau,\xi_{ss})-z_{ss}^{\infty}(u,\xi_{ss})| &\le Ce^{-\sigma^{ss}(\tau-u)}, \\ |z_s(u,\tau,\xi_{ss})-z_s^{\infty}(u,\xi_{ss})| &\le Ce^{-\sigma^{s}(\tau-u)}. \end{aligned}$$

As in the proof of Lemma B.3, we simplify the notation and write for example $z_{ss}(t)$ for $z_{ss}(t,\tau,\xi_{ss})$. We have

$$
\begin{aligned}
z_{ss}(u) &= e^{(2\beta-\alpha)(\tau-u)}\xi_{ss} + \int_0^{\tau-u} e^{(2\beta-\alpha)(\tau-u)} e^{\alpha s} F^{ss}(x(s))ds, && (16)\\
z_s(u) &= 1 + \int_0^{\tau-u} e^{\beta s} F^s(x(s))ds. && (17)
\end{aligned}
$$

One computes that

$$
\begin{aligned}
\frac{\partial}{\partial\tau} z_{ss}(u) &= (2\beta-\alpha)e^{(2\beta-\alpha)(\tau-u)}\xi_{ss} + e^{2\beta(\tau-u)}F_{ss}(x(\tau-u))\\
&\quad + \int_0^{\tau-u}(2\beta-\alpha)e^{(2\beta-\alpha)(\tau-u)}e^{\alpha s}F_{ss}(x(s))ds\\
&\quad + \int_0^{\tau-u} e^{(2\beta-\alpha)(\tau-u)}e^{\alpha s}\frac{\partial}{\partial\tau}F_{ss}(x(s))ds, && (18)\\
\frac{\partial}{\partial\tau} z_s(u) &= e^{\beta(\tau-u)}F^s(x(\tau-u)) + \int_0^{\tau-u} e^{\beta s}\frac{\partial}{\partial\tau}F^s(x(s))ds. && (19)
\end{aligned}
$$

Lemma B.3 yields

$$
\begin{aligned}
|F^{ss}(x(s))| \le C_0 e^{-3\beta s}, &\qquad \left|\frac{\partial}{\partial\tau}F^{ss}(x(s))\right| \le C_0 e^{-3\beta s+(s-\tau)},\\
|F^{s}(x(s))| \le C_0 e^{-2\beta s}, &\qquad \left|\frac{\partial}{\partial\tau}F^{s}(x(s))\right| \le C_0 e^{-2\beta s+(s-\tau)}.
\end{aligned}
$$

Direct estimates now prove (14) and (15), compare [Den89b]. Estimates for derivatives are obtained similarly, by differentiating (16) and (17). □

The above lemmas yield expansions

$$
\begin{aligned}
x_{ss}(\tau,\tau,\xi_s) &= e^{-2\beta\tau}\left(\psi^{ss}(\xi_s) + T^{ss}(\xi_s,\tau)\right), && (20)\\
x_{s}(\tau,\tau,\xi_s) &= e^{-\beta\tau}\left(\psi^{s}(\xi_s) + T^{s}(\xi_s,\tau)\right). && (21)
\end{aligned}
$$

Here T^{ss} and T^s as well as their derivatives are of order $\mathcal{O}(e^{-\sigma^{ss}\tau})$ and $\mathcal{O}(e^{-\sigma^{s}\tau})$, respectively, as $\tau\to\infty$. $x_u(0,\tau,\xi_s) = e^{-\tau} = 1$ we get $\tau = -\ln x_u$. Putting this in the expansion formulas (20), (21) for $x_{ss}(\tau,\tau,\xi_s)$ and $x_s(\tau,\tau,\xi_s)$ gives the result of Proposition B.2. □

B.2 Exponential expansions for the orbit-flip

Recall that $\Sigma^{in} = \{x_{ss} = 1\}$ and $\Sigma^{out} = \{x_u = 1\}$. Asymptotic expansions for the local transition map $\Phi_{loc} : \Sigma^{in} \to \Sigma^{out}$ are derived using analogous techniques as in the previous section. In [HKN97] such expansions are given for the case $1 < \beta < 1/2$.

Proposition B.5 *After a smooth local coordinate change, $\Phi_{loc} : \Sigma^{in} \to \Sigma^{out}$ has the following expression for its components $\Phi_{loc} = (\Phi^{ss}_{loc}, \Phi^{s}_{loc})$:*

$$\begin{aligned} \Phi^{ss}_{loc}(x_s, x_u) &= x_u^\alpha \left(\psi^{ss}(x_s) + R^{ss}(x_s, x_u)\right) + x_s x_u^\beta U^{ss}(x_s, x_u), \\ \Phi^{s}_{loc}(x_s, x_u) &= x_s x_u^\beta \left(\phi^{s}(x_s) + U^{s}(x_s, x_u)\right) + x_u^\alpha \left(\psi^{s}(x_s) + R^{s}(x_s, x_u)\right). \end{aligned}$$

The functions $\psi^s, \phi^{ss}, \phi^s$ are smooth, $\psi^{ss}, \phi^s \neq 0$.

Furthermore, R^{ss}, R^s, U^{ss}, U^s are smooth for $x_u > 0$; for some $\sigma > 0$, there exist constants $C_{k+l} > 0$ so that, with $i = ss, s$

$$\begin{aligned} \left| \frac{\partial^{k+l}}{\partial x_u^k \partial (x_s, \mu)^l} R^i(x_s, x_u) \right| &\leq C_{k+l} x_u^{\sigma - k}, \\ \left| \frac{\partial^{k+l}}{\partial x_u^k \partial (x_s, \mu)^l} U^i(x_s, x_u) \right| &\leq C_{k+l} x_u^{\sigma - k}. \end{aligned}$$

□

Proof. We merely indicate the strategy. Performing estimates as before, one shows that, for some $\omega > 0$, $\Phi^{ss}_{loc} = \mathcal{O}(x_u^{\beta+\omega})$ and $\Phi^{s}_{loc} = x_u^\beta \phi(x_s) + \mathcal{O}(x_u^{\beta+\omega})$.

For $x_s = 0$, better expansions can be obtained. Consider the orbit $(x_{ss}, x_s, x_u)(t, \tau)$ with $x_{ss}(0) = 1$, $x_s(0) = \xi_s$ and $x_u(\tau) = 1$. If $\xi_s = 0$ then the variation of constants formula yields

$$\begin{aligned} x_{ss}(t, \tau) &= e^{-\alpha t} + \int_0^t e^{-\alpha(t-s)} F^{ss}(x(s)) ds, \\ x_s(t, \tau) &= \int_0^t e^{-\beta(t-s)} F^{s}(x(s)) ds, \end{aligned}$$

where we have written $x(s) = (x_{ss}, x_s, x_u)(s, \tau)$. By performing estimates as before, one derives from these formulas that for some $\omega > 0$, $\Phi^{ss}_{loc} = c x_u^\alpha + \mathcal{O}(x_u^{\alpha+\omega})$ and $\Phi^{s}_{loc} = d x_u^\alpha + \mathcal{O}(x_u^{\alpha+\omega})$. Here c and d are smooth function of μ with $c \neq 0$.

Combining the two estimates for general x_s and for $x_s = 0$ implies the result. □